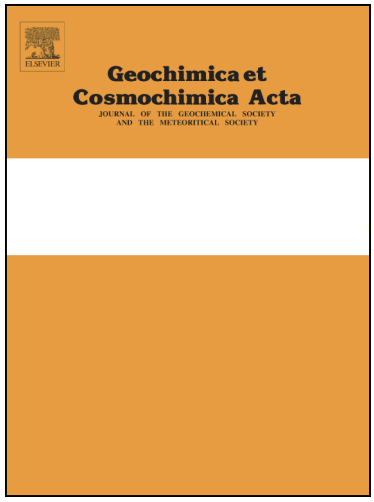

Abiotic and biotic controls on methane formation down to 2.5 km depth within the Precambrian Fennoscandian Shield

Riikka Kietäväinen, Lasse Ahonen, Paula Niinikoski, Hannu Nykänen, Ilmo T. Kukkonen

PII: S0016-7037(16)30729-3
DOI: http://dx.doi.org/10.1016/j.gca.2016.12.020
Reference: GCA 10072

To appear in: *Geochimica et Cosmochimica Acta*

Received Date: 10 February 2016
Revised Date: 18 November 2016
Accepted Date: 13 December 2016

Please cite this article as: Kietäväinen, R., Ahonen, L., Niinikoski, P., Nykänen, H., Kukkonen, I.T., Abiotic and biotic controls on methane formation down to 2.5 km depth within the Precambrian Fennoscandian Shield, *Geochimica et Cosmochimica Acta* (2016), doi: http://dx.doi.org/10.1016/j.gca.2016.12.020

Abiotic and biotic controls on methane formation down to 2.5 km depth within the Precambrian Fennoscandian Shield

*Riikka Kietäväinen[a], Lasse Ahonen[a], Paula Niinikoski[b], Hannu Nykänen[c]1 and Ilmo T. Kukkonen[a]2

[a]Geological Survey of Finland (GTK), P.O. Box 96, FI-02151 Espoo, Finland
e-mail: riikka.kietavainen@gtk.fi; lasse.ahonen@gtk.fi

[b]University of Helsinki, Department of Geosciences and Geography, P.O. Box 64, FI-00014 Helsinki, Finland
e-mail: paula.niinikoski@helsinki.fi

[c]University of Jyväskylä, Department of Biological and Environmental Sciences, P.O. Box 35, FI-40014 University of Jyväskylä, Finland

[1]Present address: University of Eastern Finland, Department of Environmental Science, P.O.Box 1627, FI-70211 Kuopio, Finland
e-mail: hannu.nykanen@uef.fi

[2]Present address: University of Helsinki, Department of Physics, P.O.Box 64, FI-00014 Helsinki, Finland
e-mail: ilmo.kukkonen@helsinki.fi

*Corresponding author:
Telephone: +358 (0)50 348 8001

Abstract

Despite a geological history characterized by high temperature and pressure processes and organic carbon deprived crystalline bedrock, large amounts of hydrocarbons are found in deep groundwaters within Precambrian continental shields. In many sites, methane comprises more that 80% of the dissolved gas phase reaching concentrations of tens of mmol l^{-1}. In this study, we used isotopic methods to study the carbon isotope systematics and sources of crustal methane within the Fennoscandian Shield. The main study sites were the Outokumpu Deep Drill Hole and the Pyhäsalmi mine in Finland, both of which allow groundwater sampling down to 2.5 km depth and have been previously studied for their groundwater chemistry and microbiology. We show that the differences in the amount and isotopic composition of methane are related to the availability of carbon sources as well as processes behind the incorporation of hydrogen and carbon via abiotic and biotic pathways into hydrocarbon molecules. Supported by previously reported occurrences and isotopic data of deep groundwater methane in lithologically different locations in Finland and Sweden, we show that methane formation is controlled by microbial methanogenesis and abiotic reactions, as well as lithology with the metasedimentary environments being the most favourable for methane occurrence. Rather than a thermogenic relic, crustal methane within the Fennoscandian Shield is more likely the result of low temperature formation from ancient organic compounds or their inorganic intermediates such as graphite. Such crustal gases are characterized by the lack of major amounts of C_2+ hydrocarbons and ^{13}C rich methane. Further, microbiological and isotopic geochemical evidence suggest that microbial methane is more common at depths shallower than 1.5 km.

Keywords: Methane, ethane, hydrogen, carbon isotopes, calcite, graphite, Fennoscandian Shield, Outokumpu, Pyhäsalmi

1. INTRODUCTION

Methane (CH_4) is a key component in the interface of geological and biological i.e. abiotic and biotic world. Deep saline groundwaters within Precambrian continental shields are among the most peculiar environments where CH_4 has been found, sometimes at vast amounts exceeding 80% of the gas phase (e.g. Sherwood et al., 1988; Ward et al., 2004; Pitkänen and Partamies, 2007; Stotler et al., 2010). The information on processes generating CH_4 and their relative abundance in crystalline bedrock environment is important in evaluating the energetic limitations of microbial life in deep dark biosphere as well as microbe-water-rock interactions. These processes are important in understanding the evolution of life on Earth as well as potential for life on other planets. More practical applications include assessment of groundwater quality, safety of geological disposal of nuclear waste, and deep mining as water-rock interaction and microbial attainment may have an impact on the environment by changing the concentrations or mobility of potentially hazardous or corrosive compounds.

In deep subsurface environments CH_4 is known to be formed via three main mechanisms: 1) thermogenically by breakdown of organic matter, 2) microbially, and 3) abiotically from reactions of inorganic compounds such as CO_2 and H_2 (Kotelnikova, 2002; Etiope and Sherwood Lollar, 2013; Sephton and Hazen, 2013; Kietäväinen and Purkamo, 2015). Microbial methanogenic processes are commonly divided into autotrophic and heterotrophic pathways which utilize inorganic and organic carbon sources, respectively (Kotelnikova, 2002; Kietäväinen and Purkamo, 2015). The most commonly examined abiotic formation mechanism is the Fischer-Tropsch type (FTT) synthesis, i.e. the catalytic formation of CH_4 from CO and H_2 at high temperature, and its proposed natural analogues (e.g. Anderson, 1984; Horita and Berndt, 1999; Sherwood Lollar et al., 2002; Taran et al., 2007; Jacquemin et al., 2010; Zhang et al., 2013). Other abiotic reactions possibly capable of producing hydrocarbons include thermal decomposition of carbonate minerals, abiotic synthesis from carbon-bearing fluids and sulphide minerals through organosulphur intermediates (e.g. thiols), and clay catalysed synthesis (McCollom, 2013). In deep drill holes, such as the 6.6 km deep Gravberg-1 (Siljan Ring) in Sweden and 9 km deep KTB (Kontinentales Tiefbohrprogramm) in Germany, artificial CH_4 formed in reactions promoted by high temperature at the drill bit - rock interface (bit-metamorphism) has also been observed (Jeffrey and Kaplan, 1988; Faber et al., 1999).

Despite the drastic differences in the formation mechanisms, the separation of different sources of CH_4 is not a trivial task. Traditional classification diagrams for CH_4 such as those by Schoell (1980, 1988) and Whiticar (1999) were mainly based on isotope data from sedimentary and surface environments where organic compounds are ubiquitous. However, deep groundwaters in crystalline bedrock differ greatly from these environments because inorganic and refractory carbon sources dominate and even dissolved inorganic carbon (DIC) is often scarce (e.g. Kietäväinen and Purkamo, 2015 and references therein). Based on the increasing amount of data from crystalline bedrock, modifications have been made to these classical diagrams (e.g. Etiope et al., 2013; Etiope and Schoell, 2014) that now also include abiotic CH_4 of different origins. In addition, approaches have been made to use other parameters such as the combination of isotopic and compositional data (Bernard et al., 1976), and the change of isotopic composition with carbon number, i.e. with the chain length of alkanes (e.g. Sherwood Lollar et al., 2008; Burruss and Laughrey, 2010). Still, the basis of these classifications has in many cases been insufficient to reliably separate between different sources of CH_4 but in a very broad sense.

On one hand this is because the isotopic composition of a product gas, whether abiotic or biotic, is heavily dependent on the isotopic composition of the reactants/substrates (e.g. Schoell, 1983; Kotelnikova, 2002). On the other hand, the isotopic compositions are dependent on such factors as openness of the system, equilibration, time scale, and substrate limitation or excess (Burke, 1993; Whiticar, 1999; Valentine et al., 2004; Kelley et al., 2012; Reeves et al., 2012; Suda et al., 2014). However, these conditions are often poorly known. Therefore it is important to study the relevant chemical components as well as their isotopic compositions in order to get a view of gas generating processes in a given system. In addition, the information on lithology, microbiology and hydrogeology is essential in judging between the different processes.

We selected two lithologically different sites within the Precambrian crystalline bedrock in Finland within the Fennoscandian Shield for a detailed study of hydrocarbons. In the Outokumpu Deep Drill Hole, characterized by metasediments and ophiolite-derived serpentinites, CH_4 typically comprises over 70 vol-% of the dissolved gas phase with concentrations as high as 32 mmol l^{-1} (Kietäväinen et al., 2013). Methane producing as well as consuming microorganisms have been found from the drill hole and fracture waters (Itävaara et al., 2011; Purkamo et al., 2015a, 2015b). Residence times of

groundwater up to 58 Ma (Kietäväinen et al., 2014) make this one of the oldest known ecosystems on Earth. In addition to dissolved carbon and carbonates, possible sources of carbon in the bedrock include graphite-rich black schist. Serpentinites provide a potential source of H_2 needed in both abiotic CH_4 synthesis and microbial methanogenesis (Devirts et al., 1993; McCollom and Bach, 2009; Neubeck et al., 2011; Schrenk et al., 2013), and radiolytic H_2 (Vovk 1987; Lin et al., 2005a, 2005b) may be present. In the Pyhäsalmi mine, ca. 180 km northwest from Outokumpu, the dominant lithologies are felsic to mafic metavolcanic rocks and granite. At Pyhäsalmi, CH_4 is scarcer, with a maximum concentration no higher than 0.55 mmol l^{-1}, but H_2 is abundant (Miettinen et al., 2015). In contrast to Outokumpu, volcanic rocks of Pyhäsalmi lack evident carbon source minerals. Yet, there are indications of CH_4 producing archaea living in the formation fluids of Pyhäsalmi at least down to 2.4 km depth (Miettinen et al., 2015).

In this study we use the isotopic compositions of hydrogen, carbon and oxygen in CH_4, ethane (C_2H_6), propane (C_3H_8), DIC, calcite, graphite, molecular hydrogen (H_2) and water, together with information on gas compositions determined from the Outokumpu Deep Drill Hole and Pyhäsalmi mine fluid samples to determine CH_4 generating processes down to a depth of 2.5 km. To ascertain the representativeness of the samples, different sampling methods are also compared. A regional scale is brought up by comparing the results of this study to previously reported isotopic compositions of CH_4 in deep groundwaters in Finland (Heikkinen, 1972; Hyyppä, 1981; Sherwood Lollar et al., 1993a, 1993b; Haveman et al., 1999, Pitkänen and Partamies, 2007) and Sweden (Jeffrey and Kaplan, 1988). The aim is to reveal possible systematics of CH_4 occurrence and isotopic composition in relation to depth, as well as lithological, physicochemical and microbiological factors in order to gain better understanding on the deep carbon cycle.

2. STUDY SITES

The Outokumpu Deep Drill Hole is located in eastern Finland (62°43′02.63″N, 29°03′55.01″E) within the Fennoscandian Shield (Fig. 1). It reaches a maximum depth of 2516 m, which makes it the deepest scientific drill hole in Finland and one of the deepest within the whole Fennoscandian Shield. The 1.9 billion year old bedrock at the study site is mainly comprised of amphibolite facies (550 – 675°C at 3 – 5 kbar) metasediments, i.e. mica schist and biotite gneiss, which are interlayered with ophiolitic rocks

of the Outokumpu assemblage and dissected by slightly younger granitoids (Fig. 1, Claesson et al., 1993; Säntti et al., 2006; Peltonen et al., 2008; Lahtinen et al., 2010; Västi, 2011).

Graphite is common as disseminated grains and black schist layers in mica schist. Occurrence of organic carbon (kerogen and traces of bitumoids) in the black schist has also been reported (Taran et al., 2011). The thickest black schist layers are found in relation with the Outokumpu assemblage between 1300 – 1600 m depth in the drill hole section and were suggested to be deposited under anoxic conditions at the margin of the Karelian Craton which was steadily sinking due to a collision with the Svecofennian (1.93 - 1.91 Ga) arc complex (Kontinen et al., 2006; Loukola-Ruskeeniemi, 1999). In addition to black schist, the Outokumpu assemblage rocks present in the Outokumpu deep drill core consist of ophiolite-derived serpentinites, calc-silicate rocks (skarn) and quartz rocks (Västi, 2011). For a long time the calc-silicate and quartz rocks at Outokumpu were interpreted as sedimentary in origin (e.g. Park, 1988; Karhu, 1993). However, their trace element composition, most notably high contents of chromium and nickel, resemble those of the serpentinites, pointing out their origin by metasomatic alteration of mantle material (Peltonen et al., 2008). Dolomitic carbonate rocks of the Outokumpu assemblage have $\delta^{13}C$ values between +0‰ and -3‰ VPDB (Karhu, 1993; Kontinen et al., 2006). The highest values are interpreted to represent seawater-derived inorganic carbon, probably introduced in the form of carbonate clasts embodied in turbidites or directly from circulating seawater (Kontinen et al., 2006).

Saline water with the concentration of total dissolved solids (TDS) as high as 70 g l^{-1} enters the Outokumpu Deep Drill Hole along fracture zones which are separated from each other by tens to hundreds of meters of impermeable rock (Ahonen et al., 2011; Kietäväinen et al., 2013). A major divide in groundwater composition is seen at around 1300 m depth where the salinity suddenly increases, water and strontium becomes more enriched in the heavier isotopes and the concentration of CH_4 decreases while the proportion of H_2 begins to increase (Kietäväinen et al., 2013). Likewise there is a change in the microbial community structure which seems to closely mirror the change in groundwater chemistry, and lithology (Itävaara et al., 2011; Kietäväinen et al., 2013; Nyyssönen et al., 2014; Purkamo et al., 2013, 2015a, 2015b). The Outokumpu Deep Drill Hole groundwater is isolated from the modern meteoric water cycle and both water stable isotopes and noble gases indicate residence times of tens of millions of years (Kietäväinen et al., 2013, 2014). Any contribution of mantle

187 degassing in the Outokumpu fluids can be excluded based on the crustal $^{3}He/^{4}He$ ratios of 1-2 • 10^{-8}
188 (Kietäväinen et al., 2014).
189
190 In addition to an extensive sampling campaign at Outokumpu, samples were also taken from the
191 Pyhäsalmi mine located ca. 180 km northeast from Outokumpu (63°39'N, 26°03'E) along the boundary
192 between the Proterozoic and Archaean parts of the Fennoscandian Shield (Fig. 1). The Pyhäsalmi mine
193 is in a volcanogenic massive sulphide (VMS) type Cu-Zn deposit and among the deepest metal mines
194 in Europe. The deepest hole (R-2247) drilled downwards from the 1430 m depth level of the mine
195 reach the depth of 2400 m below the surface (Fig. 1). Dominant rock types are 1.92 Ga old mafic to
196 felsic volcanites which have metamorphosed at amphibolite facies conditions similar to Outokumpu,
197 with minor occurrence of slightly younger granite (Kousa et al., 1994; Miettinen et al., 2015). Salinity
198 of groundwater increases with depth reaching the TDS concentration of 76 g l^{-1} at 2400 m (Miettinen et
199 al., 2015). Both acidic and basic waters in the shallow and deep parts of the mine, respectively, host
200 liveable microbial communities (Kay et al., 2014; Miettinen et al., 2015).
201
202 **3. MATERIAL AND METHODS**
203
204 Sampling for geochemical analysis, including the stable isotopic composition of water, has been
205 described in Kietäväinen et al. (2013), Purkamo et al. (2013), Rajala et al. (2015) and Miettinen et al.
206 (2015). The overall geochemical characterisation of the Outokumpu Deep Drill Hole and the Pyhäsalmi
207 mine groundwaters has been previously published in Kietäväinen et al. (2013) and Miettinen et al.
208 (2015), respectively. Isotopic compositions of graphite from Outokumpu are provided by Taran et al.
209 (2011). Here we focus on describing the sampling and isotopic analysis of gases and dissolved
210 inorganic carbon (DIC) as well as fracture carbonates.
211
212 **3.1 Fluid sampling**
213
214 Gas samples from the Outokumpu Deep Drill Hole were taken between 2010 and 2012, and cover a
215 depth range from 180 to 2480 m below the surface (bsl). In the Pyhäsalmi mine samples for isotopic
216 analysis of gases were taken in 2014 from two drill holes (R-2247 and R-2227) starting from the mine
217 level of 1430 m bsl and extending down to 2400 m depth. At Outokumpu, five different sampling

methods were used (Table 1): 1) tube sampling with 100 m sections (Nurmi and Kukkonen, 1986), 2) direct pumping, 3) pumping with packers (Ahonen et al., 2011), 4) "PAVE" pressurised sampling device (Haveman et al., 1999; Ahonen et al., 2011), and 5) Leutert positive displacement sampler (PDS; Regenspurg et al., 2010; Kietäväinen et al., 2013, 2014). Samples from the Pyhäsalmi mine were taken from free flowing fluid as described in detail by Miettinen et al. (2015).

From the tube sampler and pumped fluid the samples for gas analyses were taken either by injecting the spontaneously separated gas into head space bottles or diverting the gas into inverted glass bottles (Schott) under sample water ("a bucket method"). In both cases the bottles were flushed with argon and filled with sample water prior to gas collection in order to avoid contamination with air. In these samples some sample water was usually left in the bottles to prevent diffusion through the septa. From the "PAVE" samples (180 m depth) gas was directly released into analysis in the lab, whereas from the PDS, gas was collected into evacuated gas sampling bulbs in a vacuum line and gas separation assisted by heating in an ultrasonic bath in the field (Kietäväinen et al., 2013, 2014). The gas samples were not fixed, except one sample from Pyhäsalmi (PYS-1B) in which a few grains of solid $HgCl_2$ were added before the evacuation and gas injection. However, microbial activity can be considered minimal for the gas–only (dry) samples which include the PDS samples from Outokumpu and samples taken by the injection method in the Pyhäsalmi mine (method FFI in Table 2 and Table EA 1).

The samples for DIC isotope analyses were taken from the Outokumpu Deep Drill Hole in 2010 and 2011. In 2010 DIC isotope samples from pumped fluid from 500 and 2260 m depths were collected into LABCO Exetainer tubes (12 ml), which contained 0.15 ml of 85% phosphoric acid and were flushed and filled with He (purity > 99,996%). During sampling 5 ml of He was removed and 8 ml of sample water immediately injected into each tube. From the tube sampling in October 2011 the samples were collected in evacuated glass bottles (60 ml), specially manufactured to fit the caps from Vacutainer vials. The bottles were prepared by adding 3 ml of 85% phosphoric acid and a magnetic rod and evacuating them on a vacuum line specially designed for extracting DIC from water samples. The sample preparation was done at the Geological Survey of Finland (GTK) in Espoo. Samples for DIC isotope analysis were injected into evacuated glass bottles through a 0.8/0.2 µm supor membrane filter using a plastic syringe. Vials and tubes were stored upturned in dark and cool until analysed.

3.2 Sample selection and preparation for fracture mineral studies

In total, 58 rock samples along the Outokumpu deep drill core were selected between 100.90 and 2240.70 m depths below the surface. Samples represent both open and sealed fractures and thin veins. Ordinary 30 µm thick polished thin sections were prepared for microscopy and microanalysis studies. Loose fracture fillings were fixed with epoxy resin before cutting. In the case of extremely loose fillings, thin sections were not possible to make and, instead, minerals were mounted on a carbon tape. Calcites for isotopic analysis were carefully selected under a microscope and separated using a steel blade. Where different calcite generations occurred, they were sampled separately. Fractures dissected by the drill holes studied at Pyhäsalmi did not contain carbonate minerals (Miettinen et al., 2015).

3.3 Analysis

3.3.1 Dissolved gases

The gas composition was analysed by gas chromatography at Ramboll Analytics (Vantaa, Finland) or Isotech Laboratories (Illinois, USA) (Kietäväinen et al., 2013; Miettinen et al., 2015). Within the whole sample set (Table EA 1), relative uncertainties were generally better than 8% for hydrocarbons, 3% for H_2, 4% for O_2 and N_2, 6% for CO_2, and 10% for He and Ar.

The isotopic compositions of CH_4, C_2H_6 and from few samples also C_3H_8 from Outokumpu were determined at the Environmental Isotope Laboratory at the University of Waterloo (Ontario, Canada). Samples from the Pyhäsalmi mine were analysed for their isotopic composition at Isotech Laboratories. Following the separation by Trace Ultra Gas Chromatograph (Thermo Finnigan) the different hydrocarbons were converted to CO_2 at 940ºC and to H_2 at 1450°C and analysed with a Delta^{plus} XL isotope ratio mass spectrometer (Thermo Finnigan MAT). The isotopic compositions are reported using δ-notation per mill (‰) relative to VPDB (Vienna Pee Dee Belemnite) and VSMOW (Vienna Standard Mean Ocean Water) standards for C and H, respectively:

$$\delta\,(‰) = \left(\frac{R_{sample}}{R_{standard}} - 1\right) * 1000 \qquad (1)$$

where R is either $^{13}C/^{12}C$ or $^{2}H/^{1}H$.

Analytical error is estimated to be ±0.5‰ for $\delta^{13}C$ and ±7‰ for $\delta^{2}H$. The isotopic composition of H_2 gas was analysed from three Outokumpu samples in Hydroisotop GmbH (Schweitenkirchen, Germany) with the analytical uncertainty of ± 10‰.

3.3.2 Isotopic composition of dissolved inorganic carbon

Isotopic analyses of DIC samples from 2011 were conducted at the Department of Geosciences and Geography at the University of Helsinki as follows. Before isotopic analysis the DIC samples in Vacutainer-fitted vials were heated to 50°C and attached to the vacuum line and CO_2 extracted and collected into Exetainer vials as described by Atekwana and Krishnamurthy (1998). The extraction time was 2 x 10 minutes. The samples were injected with helium before analysing them on an isotope ratio mass spectrometer (Thermo Finnigan Delta Plus Advantage) using laboratory standards calibrated against an international standard (VPDB). The absolute uncertainty of the DIC isotope analysis with this method was ≤ 0.60‰ at 1σ level. DIC samples from the pumped fluid from 500 and 2260 m depths were analysed at the University of Jyväskylä with a Gas-Bench II connected to a Thermo Finnigan XP Advantage, using international measurement standard NBS 19 calcite and an in-house carbon standard, $CaCO_3$. In this case the reproducibility of the standard measurements was 0.09‰ at 1σ level (n= 3). The results are reported using δ-notation (Eq. 1) relative to VPDB standard.

3.3.3 Characterisation of fracture minerals

Fracture mineralogy was studied using both optical and scanning electron microscopy (SEM/ JEOL JSM-5900LV) at the Geological Survey of Finland (GTK) in Espoo. High vacuum, energy dispersive (EDS) mode with voltage of 20 kV and spot size of 50 µm was used during the SEM analysis for carbon coated thin sections. Low vacuum mode was used for uncoated samples on carbon tape.

3.3.4 Stable isotopes of calcite

Approximately 150 µg of calcite sample was weighted into Exetainer vials and reacted with concentrated phosphoric acid for at least 1 h at 70ºC. Carbon and oxygen stable isotopes were analysed from the released CO_2 gas by Thermo Finnigan Delta Plus Advantage gas source mass spectrometer at the University of Helsinki, Department of Geosciences and Geography. To test reproducibility of the analysis, an in-house calcite reference was regularly analysed among the samples. The results are

reported using δ-notation (Eq. 1) relative to VPDB standard for both carbon ($R = {}^{13}C/{}^{12}C$) and oxygen ($R = {}^{18}O/{}^{16}O$). The reproducibility was ±0.07‰ for $\delta^{13}C$ and ±0.12‰ for $\delta^{18}O$ at 1σ level (n=20).

3.4 Computational methods

The speciation and concentrations of dissolved inorganic carbon (DIC) and saturation index (SI) of calcite was calculated using the PHREEQC software, "wateq4f" database (USGS, 2014). A saturation index is determined as follows:

$$SI = \log\frac{Q}{K} \quad (2)$$

where Q is the ion activity product and K is the thermodynamic reaction constant (Clark and Fritz, 1997). In equilibrium SI equals 0 while positive and negative SI values indicate oversaturation and undersaturation (dissolution), respectively. *In situ* temperatures measured from the Outokumpu Deep Drill Hole (Kukkonen et al., 2011) and on site at the Pyhäsalmi mine (Miettinen et al., 2015) were used in all calculations. The hydrostatic pressure increase of about 100 bar km^{-1} was not taken into account as 1 bar pressure is used by the PHREEQC by default. Increased pressure will increase the solubility of calcite especially at low temperatures (Duan and Li, 2008) and may lead to slight overestimation of the saturation indices presented here. Additionally, high ionic strength of saline waters causes uncertainty in defining thermodynamic activity product (Q) of dissolved species. The field or on-line measurements of pH and alkalinity were used when available, as the pH was observed to rapidly decrease in contact with air apparently due to the dissolution of atmospheric CO_2 into these low alkaline waters with poor buffering capacity.

Isotopic fractionation factors (α) between phases x and y were calculated according to Eq. 3:

$$\alpha_{x-y} = \frac{1000 + \delta x}{1000 + \delta y} \quad (3)$$

where δ refers to the determined isotopic compositions in ‰ relative to standard (Eq. 1). The correlation between α and temperature (T, in Kelvin) is:

$$ln\alpha_{x-y} = aT^{-2} + bT^{-1} + c \quad (4)$$

Isotopic separation (Δ) between phases x and y is simply the difference in their δ-values:

$$\Delta_{x-y} = \delta_x - \delta_y \quad (5)$$

4. RESULTS

4.1 Gas composition

A compilation of gas data, including sampling depths and methods, collected from the Outokumpu Deep Drill Hole and the Pyhäsalmi mine is given in the Electronic Annex (Table EA1). CH_4 and N_2 are by far the most abundant dissolved gases at Outokumpu, while H_2 becomes dominant in the deepest part of the drill hole. At Pyhäsalmi the gas phase is dominated by N_2 and He. The PDS samples from 500 and 2480 m depths and the sample PYS-2 from the Pyhäsalmi mine have suffered from severe air contamination (O_2 > 5 vol-%), but some O_2 is present in virtually all samples. The pressurised samples are relatively enriched in H_2 and He and depleted in CH_4 compared to samples obtained by pumping, the tube sampler or from free flowing fluid in the mine. At Outokumpu $CH_4/(C_2H_6 + C_3H_8)$ ratio varies from 71 to 333 (Table EA1), such that a decrease is observed towards the surface. At Pyhäsalmi CH_4/C_2+ ratios are typically < 10, with only one drill hole (R-2250) having a significantly higher ratio of 164 (Table EA1). Ethene, propene and butene were below analytical detection (0.001 vol-%) in all samples.

4.2 Isotopic composition of gases

The isotopic compositions of CH_4, C_2H_6, C_3H_8 and H_2 are given in Table 2. Variation in the isotopic composition of CH_4 is large from -404 to -136‰ VSMOW for δ^2H_{CH4} and from -39.9 to -13.2‰ VPDB for $\delta^{13}C_{CH4}$, although most samples have δ^2H_{CH4} around -280‰ VSMOW and $\delta^{13}C_{CH4}$ around -30‰ VPDB (Fig. 2). ^{13}C depleted and ^2H enriched CH_4 is unique for the depth of 1470 m at Outokumpu and ^{13}C enriched and ^2H depleted CH_4 is only found below 2260 m depth. The minimum and maximum values of δ^2H_{CH4} and $\delta^{13}C_{CH4}$ are generally those from the pressurised samples (PDS and

PAVE). However, the isotopic compositions are not systematically shifted compared to the tube samples.

Similarly to CH_4, the most ^{13}C enriched C_2H_6 is found from the 2480 m depth at Outokumpu and deep samples from the Pyhäsalmi mine. A fracture zone at 180 m depth has distinctive δ^2H_{C2H6} values as heavy as -152‰ VSMOW, while the other samples have δ^2H_{C2H6} around -250‰ VSMOW (Table 2). Isotopic data of C_3H_8 are only available for carbon from two depths from Outokumpu (500 and 2260 m) and only pumped fluids are represented. Nevertheless, the isotopic composition of carbon seems to be systematically lighter from CH_4 to C_3H_8 and C_2H_6, except samples from tube sampling in May 2011 which, with no apparent reason, show anomalously ^{13}C rich values of C_2H_6 (Table 2). This indicates a $\delta^{13}C$ vs. carbon number trend is V-shaped (Fig. 3) rather than normal (ascending) or inversed (declining), i.e. neither of the two trends which have often been related to thermogenic and FTT type abiotic hydrocarbons, respectively (e.g., Sherwood Lollar et al., 2002; Etiope and Sherwood Lollar, 2013; Zhang et al., 2013). Hydrocarbons at Pyhäsalmi seem to differ from this pattern as they show enrichment of ^{13}C in C_2H_6 over CH_4 (Fig. 3).

Molecular hydrogen is extremely depleted in deuterium with the measured isotope range from -798 to -727‰ VSMOW at Outokumpu and from -736 to -680‰ VSMOW at Pyhäsalmi. While the addition of $HgCl_2$ into one of the gas samples from Pyhäsalmi (PYS-1B) did not affected the C or H isotopic composition of CH_4, the δ^2H value of H_2 was 56‰ higher in the fixed sample compared to the untreated sample taken at the same time (Table 2). This one control with eliminated biological activity is clearly not enough for making generalised conclusions on the possible microbial processes during sample storage. However, there was no difference in the concentration of H_2 between the comparative samples which could indicate microbial production or consumption of H_2 (Table EA1).

4.3 Dissolved inorganic carbon

The modelled concentrations of DIC are very low (Table 2), with an average of 0.16 mmol l^{-1} at Outokumpu and only 2 µmol l^{-1} at Pyhäsalmi. Governed by pH and Ca concentration, the main constituent of DIC is HCO_3^- or $CaCO_{3(aq)}$ above and below 1500 m, respectively. The isotopic

composition of DIC varies from -18.1 to -0.8‰ VPDB with a general increase in ^{13}C with depth (Table 2, Fig. 4).

4.4 Fracture mineralogy

At Outokumpu saturation indices (SIs) of calcites at the ambient temperature and 1 bar pressure typically vary from 0.5 to 1.5 and only the two PDS samples from 1470 m depth show slightly negative SI values (down to -0.12) which are indicative of possible dissolution of calcite. At Pyhäsalmi, however, SI values for calcites are mostly negative as is also demonstrated by the absence of calcites on the fracture surfaces. Except the few more coarse grained (mm sized) crystals found from around 500 m depth (Table 3), calcite occurs as fine, powdery layers, thin films or medium sized crystals on fracture surfaces and veins at Outokumpu, and is typically accompanied by zeolite minerals and chlorite. Pyrite and pyrrhotite are common accessory minerals. Eu- to subhedral, box shaped crystals of calcite were most common but elongated crystals were also found (Table 3). Even though the modelled values show oversaturation of calcite throughout the studied range of compositions and depth at Outokumpu no calcite was found below 1500 m depth. Instead, the most common fracture filling minerals below 1500 m are prehnite ($Ca_2Al_2Si_3O_{10}(OH)_2$) and Ca-zeolite (laumontite; $CaAl_2Si_4O_{12}•4(H_2O)$). Overall, fractures become scarce in the deeper part of the drill hole.

4.5 Isotopic composition of calcites

The isotope geochemistry of fracture filling and vein calcites from the Outokumpu Deep Drill Hole is presented in Table 3. The $\delta^{18}O$ values range from -18.7 to -9.7‰ VPDB and the $\delta^{13}C$ values from -19.64 to -3.43‰ VPDB. Calcites associated with the Outokumpu assemblage rocks have a narrow range of carbon compositions from -9 to -5‰ VPDB. The $\delta^{18}O$ values of these calcites are more variable, although all veins/fractures containing chalcopyrite plot between -16 and -14‰ VPDB.

5. DISCUSSION

In order to understand carbon cycling in general, and CH_4 formation processes in particular, we need to know 1) what are the potential sources of hydrogen and carbon needed to build a CH_4 molecule, 2) are

434 there some physicochemical conditions or microorganisms which could affect CH_4 formation and 3) is
435 CH_4 further consumed, oxidized, polymerized or escaped? In this study we aimed to answer these
436 questions by combining isotope geochemistry of carbon and hydrogen bearing phases with information
437 on lithology and microbiology at Outokumpu and Pyhäsalmi and further extending the study to cover
438 the Fennoscandian Shield based on previously published data. First we start by discussing the different
439 sampling methods and representativeness of the data.
440
441 **5.1 Comparison of different fluid sampling methods**
442
443 In a previous study (Kietäväinen et al. 2013) good correlation was observed in the anion and cation
444 contents and composition as well as the isotopic composition of groundwater between the tube
445 sampling and PDS methods at Outokumpu. However, this study has demonstrated that in the case of
446 gases the selection of the sampling method plays a more critical role. Most notably, differences in the
447 isotopic composition of CH_4 were observed between the pressurised (PDS and PAVE) and non-
448 pressurised (tube and pumping) methods. However, the shift in the isotopic compositions was not
449 systematic with respect to sampling method. Therefore the difference cannot be explained by mass
450 dependent isotopic fractionation. For the same reason it is not likely that the changes appeared due to
451 sample storage in different kind of vials.
452
453 Based on geochemical and water stable isotope data (Kietäväinen et al. 2013), and supported by the
454 compositional data of gases (Fig. 5), up to five different water types can be discerned at Outokumpu.
455 Therefore, the tube sampling and pumping may give the average composition while the pressurised
456 methods are able to more precisely capture a fluid from a particular depth. In particular, mixing of
457 gases can be promoted by the pressure drop and release of gases during pumping and tube sampling
458 before the fluid reach the surface. Thus, the most likely explanation of the observed differences in the
459 isotopic composition of CH_4 between pressurised and non-pressurised methods is mixing of gases from
460 different fracture systems and different depths either along the drill hole or within the tube. Likewise,
461 the observed relative enrichment of H_2 and He in the pressurised samples can be explained by bubbling
462 as these gases are among the least soluble and thus will be preferentially escaped during degassing.
463 Indeed, during pumping gas compositions fluctuated in a non-linear manner which could be indicative
464 of bubble formation (Table EA1, Fig. 5). Bubbling is also observed at the well head at Outokumpu.

However, the depth at which spontaneous degassing takes place in the drill hole without pumping is likely less than 150 m based on the concentrations and solubility of the main gaseous components (Kietäväinen et al., 2014; Heikkinen 2016).

In Fig. 5 we use the CH_4/N_2 and N_2/Ar ratios and $\delta^{13}C_{CH4}$ values to compare the results obtained by the different sampling techniques and further investigate post-genetic and post-sampling processes capable of modifying the composition of the gas. The CH_4/N_2 and N_2/Ar ratios are likely governed by the organic carbon composition and content of the source (e.g. Jenden et al., 1988), and may change due to bubbling (solubility), mixing (e.g. Darrah et al., 2014) and, at very long time scales, also by the accumulation of radiogenic Ar. However, as long as only advection is considered, no isotopic fractionation should occur in these processes. Bubbling for example should change the gas composition only along the y-axis in Fig. 5c and d due to preferential partitioning of the less soluble N_2 in the gas phase, and consequential depletion in the remaining fluid. This means that samples taken during and after a bubble burst will differ in their relative gas composition but, if bubbles originate from sources with different isotope signature, may also express linear change in the isotope composition of CH_4. Diffusion will also preferentially remove N_2 but may also produce ^{13}C (and ^{2}H) depletion in the diffusing gas while the residual gas will become isotopically heavy (e.g. Prinzhofer and Huc, 1995; Schloemer and Krooss, 2004), although e.g. Fuex (1980) and Schoell (1983) have argued that diffusion related isotope effects will be negligible and may only pertain non-steady state processes, if any, on hydrocarbons. In any case, the overall isotope trend at Outokumpu which shows inverse correlation of $\delta^{2}H_{CH4}$ with $\delta^{13}C_{CH4}$, does not support modification of isotope composition of CH_4 through diffusion.

When accompanied with decrease and increase of the $\delta^{13}C_{CH4}$ value, respectively, the decrease and increase in the CH_4/N_2 ratio can also be due to methanogenesis and oxidation of CH_4, in which case no change in the N_2/Ar ratio is expected. Oxidation seems to explain the difference between the results obtained by pumping and PDS at 1820 m depth and difference in the isotopic composition of CH_4 between the drill holes R-2247 and R-2227 at Pyhäsalmi (Fig 5.c,d). However, the most ^{13}C rich CH_4 observed at Outokumpu (2480 m) cannot be explained by oxidation, most notably because of the high CH_4/C_2+ value (Table EA1), and depletion in ^{2}H (Fig. 2).

5.2 Hydrogen in the system H_2O-H_2-CH_4

Incorporation of hydrogen into the CH_4 molecule can happen either from H_2O, organic matter or H_2. Due to their lower mass and position in a CH_4 molecule, equilibration of hydrogen isotopes occurs more easily than carbon isotopes (Lyon and Hulston, 1984; Ni et al., 2011; Reeves et al., 2012). This means that hydrogen may be a more sensitive tracer for CH_4 forming processes compared to carbon. However, information carried by hydrogen on its origin may be more easily lost at geological time scales.

H_2 is a common constituent of the gas phase at both Outokumpu and Pyhäsalmi (Table EA1). In Figure 6a-b, the isotopic fractionation of hydrogen in the system H_2O-H_2-CH_4 is used to examine possible equilibration of the Outokumpu and Pyhäsalmi samples with temperature. Fractionation factors (α) given by Horibe and Craig (1995) for a temperature range 0-370ºC were used to calculate the isotopic concordance curves shown (Eq. 4). For low temperatures (< 200°C) the fractionation is best established between H_2O and H_2 while higher uncertainties are related to the equilibration of hydrogen between CH_4 and H_2 or H_2O (Horibe and Craig, 1995). Nevertheless, the results fit well with each other for this limited set of samples and indicate isotopic equilibrium at ambient, or slightly higher, temperatures (Fig. 6). Thus, CH_4 seems to have formed at equilibrium controlled reactions *in situ* or to represent gas component which has later equilibrated with H_2 and H_2O. However, when the whole sample set is considered, it is apparent that, especially in the samples obtained by the pressurised methods at Outokumpu, CH_4 is not in isotopic equilibrium with H_2O at *in situ* temperatures from 5 to 40°C (Fig. 7).

The time span needed for hydrogen isotopes to equilibrate in the system H_2O-H_2-CH_4 is not well constrained but some experimental data and approximations do exist. Using the equations for optimum 99% equilibration of ^{13}C between CO_2 and CH_4 from Giggenbach (1982) and rate constants for H_2-H_2O and H_2-CH_4 isotope exchange determined by Lécluse and Robert (1994), Suda et al. (2014) calculated that at 50°C the isotopic equilibrium between H_2 and H_2O can be attained within 100 years while the equilibration between H_2 and CH_4 would take 3000 years. The isotopic equilibration of hydrogen between H_2O and CH_4 is likely to be in the same order or slower (Lyon and Hulston, 1984; Suda et al., 2014), and has been reported for natural gas accumulations in a deep sedimentary basin (Burruss and Laughrey, 2010). Lin et al. (2005b) suggested that in natural bedrock environments, residence time of

around 1 Ma should be sufficient to equilibrate the hydrogen isotopic compositions in the system H_2O-H_2 to reflect *in situ* temperatures; the time span of which is still clearly less than the estimated residence times of groundwaters at Outokumpu between 4 and 58 Ma (Kietäväinen et al., 2014). However, in the presence of H_2 utilizing microorganisms, the equilibration of hydrogen isotopes may take place remarkably fast. In particular, sulphate reducers and methanogens, also found at Outokumpu and Pyhäsalmi (Itävaara et al., 2011; Nyyssönen et al., 2014; Purkamo et al., 2013, 2015a, 2015b; Miettinen et al., 2015), have been observed to equilibrate hydrogen isotopes between H_2O and H_2 within seconds in their metabolic processes (Romanek et al., 2003; Valentine et al., 2004).

Compared to CH_4, hydrogen isotopes of C_3H_8 can be even more readily exchanged with water and, at long time scales, the isotopic exchange may be significant also for C_2H_6 (Reeves et al., 2012). Based on the equilibrium fractionation determined by Wang et al. (2009) for H isotope exchange between H_2O and C_2H_6, which is much less temperature dependent than fractionation between H_2O and CH_4, and not as likely to be affected by microbial activity, δ^2H values below -990‰ VSMOW would be expected for C_2H_6 in equilibrium with H_2O at Outokumpu. Instead the δ^2H_{C2H6} values are between -277‰ and -153‰ VSMOW (Table 2). This suggest that, when observed, the isotopic equilibration of H in the system H_2O-H_2-CH_4 is likely controlled by other factors than the long residence time, such as microbial activity. Difference between the pressurised and non-pressurised methods may arise from technical reasons, most notably the immediate separation of gas from water, which should prevent post-sampling changes in the PDS samples.

Beyond the equilibration processes, hydrogen isotope fractionation between CH_4 and H_2O is also dependent on the relative proportion of H derived from H_2O and other sources, and therefore should differ between CO_2 reduction (H from H_2O) and acetate fermentation (H from organic matter and H_2O) pathways (Fig. 7, Sugimoto and Wada 1995; Whiticar 1999). In the case of CH_4 formation from graphite (e.g. $2C + 2H_2 = CH_4 + CO_2$, or $C + 2H_2O + 4Fe_3O_4 = 3Fe_2O_3 + CH_4$; Burruss and Laughrey, 2010), the fractionation would likely be similar to CO_2 reduction as in both cases H_2O provides the only hydrogen source. While most of the variation among the samples from Outokumpu and Pyhäsalmi may be explained by the change in the relative proportion of CO_2 reduction and acetate fermentation, values exceeding the suggested limits do occur.

Isotopic composition of CH_4 is also subject to change after the formation. Such secondary fractionation typically leads to either enrichment or depletion of both C and H isotopes in the same direction (Schoell, 1988). When accompanied with enrichment in ^{13}C (Whiticar, 1999; Etiope et al., 2011), the shift towards the less negative δ^2H_{CH4} values in Fig. 7 could be due to oxidation of CH_4. In Pyhäsalmi the more ^2H and ^{13}C enriched CH_4 from the shallower and more recently made drill hole R-2227, which contains significantly less CH_4 than the drill hole R-2247, might represent oxidised gas, possibly affected by the drilling. However, at Outokumpu the isotopic composition of CH_4 at 1470 m depth does not indicate such post-formational changes as the depletion of ^2H is coupled with enrichment of ^{13}C (Fig. 2). Instead, distinct rock types surrounding the 1470 m depth, which include serpentinite and thick layers of black schist, may provide an explanation for the different isotopic composition of CH_4. In the case of deep sourced samples, the larger isotope offset towards the more negative δ^2H_{CH4} values may be caused by the high partial pressure of H_2 (Burke 1993, Sugimoto and Wada 1995). The high $\alpha H_{H2O\text{-}CH4}$ of up to 1.56 below 2300 m depth could also be indicative of abiotic CH_4 (Sherwood Lollar et al., 2008), although high $\alpha H_{H2O\text{-}CH4}$ values have also been reported for microbial CH_4 produced by the hydrogenotrophic methanogen *Methanobacterium formicicum* (Balabane et al., 1987).

5.3 Carbon in the system CH_4-DIC-calcite-graphite

First of all, the carbon isotopic composition of CH_4 depends on the carbon source. At Outokumpu isotopic data on all phases in the system CH_4-DIC-calcite-graphite, together with additional isotopic and geochemical information such as noble gas isotopes (Kietäväinen et al., 2014) is available which allows us to study the carbon sources and sinks in detail. At Pyhäsalmi, however, the possible carbon sources are more limited and the information on the carbon isotope composition, other than that of hydrocarbons, was not studied and thus will not be discussed here.

Previously the heaviest isotopic compositions of CH_4 have been related to gases with more than 5% mantle helium (Etiope and Sherwood Lollar, 2013). However, at Outokumpu the extremely ^{13}C-rich CH_4 values found below 2300 m are associated with He which has an entirely radiogenic isotope signature (Kietäväinen et al., 2014) and thus a mantle source for the more soluble CH_4 can be excluded. Hence, the main sources of carbon include dissolved and crystalline carbonate carbon as well as refractory organic carbon, mainly graphite, within the crust.

589

590 Carbon isotopic compositions from the fracture and vein calcites in this study fall between -3 and -20‰
591 VPDB (Fig. 8a). Even though the modelled positive SI values of calcites suggest calcite precipitation
592 throughout the drill hole section, observations of calcite fillings were limited to the uppermost 1.5 km.
593 The discrepancy is likely related to the increase in the solubility of calcite with pressure which was not
594 taken into account in the model. In addition, the preservation of the latest, and probably the loosest,
595 fracture fillings may be poor because of the rotary drilling technique used. Only few of the more ^{13}C
596 depleted calcites have isotopic composition in equilibrium with the present DIC (Fig. 8a), while the
597 oxygen isotopes of calcites and present groundwater seem to be more interconnected (Fig. 8b). In part
598 the variations are likely due to different calcite generations, some of which can be remarkably old.
599 These include hydrothermal calcites which are characterised by heavy $\delta^{13}C$ values, typically above -
600 10‰ VPDB, due to preferential fractionation of ^{12}C into vapour phase (steam) during boiling in open
601 system conditions, as well as ^{18}O depleted values (Clark and Fritz, 1997; Wallin and Peterman, 1999;
602 Blyth et al., 2009). In this group belong calcites associated with the Outokumpu assemblage rocks
603 between 1300 and 1500 m depth (Fig. 8).
604
605 Several studies have also shown that carbon isotopic composition of calcites reflect changes emanating
606 from microbial activity (e.g. Pedersen et al. 1997; Blyth et al., 2009; Drake et al., 2015; Sahlstedt et al.,
607 2016). In connection with the modest $\delta^{18}O_{calcite}$ values indicative of precipitation from meteoric water
608 at varying degrees of water-rock interaction, the ^{13}C enriched values may originate from microbial
609 methanogenesis because microbes prefer ^{12}C in their metabolic reactions therefore leaving the
610 remaining DIC enriched in ^{13}C (Claypool et al., 1985; Clark and Fritz, 1997; Blyth et al., 2009). In the
611 other end, carbon input from the oxidation of CH_4 is characterised by extremely ^{13}C poor values in
612 calcites, the most ^{13}C depleted values below -15‰ VPDB thus indicating that some CH_4 derived
613 carbon was probably encountered. These occur close to the presently hydraulically active fracture
614 zones at 500 and 1000 m depths as well as in the upper 250 m (Fig. 8).
615
616 While carbon originating from the microbial oxidation of CH_4 seems to be recorded in some of the
617 calcites at active fracture zones, the source of carbon for the build-up of hydrocarbons is less evident.
618 At Outokumpu the isotopic separation (Eq. 5) between DIC and CH_4, ranges from 11 to 25‰, or
619 between ~8 and 23 ‰ if the $\delta^{13}C_{CH4}$ values of only the PDS samples are considered (Fig. 4). Although

620 the enrichment of DIC with ^{13}C can occur due to microbial methanogenesis (Claypool et al. 1985), the
621 observed simultaneous increase in $\delta^{13}C_{CH4,}$ as most clearly observed at 500 and 2260 m depths (Fig. 4,
622 does not support such isotopic evolution. Furthermore, the values of $\alpha_{CDIC\text{-}CH4}$ (< 1.025) are not
623 consistent with microbial methanogenesis through the CO_2 reduction pathway (Valentine et al., 2004;
624 Sherwood Lollar et al., 2008). However, where aceticlastic methanogens dominate the $\Delta_{DIC\text{-}CH4}$ is
625 expected to be lower, because the use of organic compounds would not directly affect the isotopic
626 composition of DIC, or abiotic reaction mechanisms may dominate. Unlike hydrogen isotopes in the
627 system H_2O-H_2-$CH_{4,}$ equilibration of carbon is more unlikely due to sluggish kinetics (Sherwood
628 Lollar et al., 2008), and thus, even though DIC and CH_4 are far from isotopic equilibrium
629 (1000lnαCHCO3-CH4 = 76.1‰ at 25°C; Clark and Fritz, 1997 after Bottinga, 1969 and Mook et al.,
630 1974) at Outokumpu, abiotic CH_4 formation from CO_2 is possible in the light of DIC isotopes.
631
632 Graphite rich black schist form another potential carbon source at Outokumpu. Compared to DIC,
633 isotopic fractionation of carbon between graphite and CH_4 is likely to be lower, as the reaction does not
634 take place through a dissolved phase. In Outokumpu, within the depth range where graphitic rocks are
635 abundant, the isotopic composition of CH_4 (Fig. 4) is very close to or only slightly depleted in ^{13}C
636 compared to graphite ($\delta^{13}C$ -27.4...-18.4‰ VPDB; Taran et al., 2011). It has been experimentally
637 shown that fractionation is lower if the starting material is graphite compared to CH_4 formation from
638 for example gaseous components (Zhang et al., 2013). This is because CH_4 formation takes place only
639 at the mineral surface where carbon isotopes are randomly dispersed (Zhang et al., 2013). Thus, notable
640 fractionation of carbon isotopes between graphite and CH_4 is not expected.
641
642 The isotopic composition of CH_4 can also depend on the amount of substrates available. The closeness
643 of the system tends significantly decrease fractionation as in the case of near-complete conversion of
644 substrates into CH_4 the isotopic fractionation could follow the Rayleigh distillation trend eventually
645 leading to minimal fractionation (Bradley et al., 2009; Kelley et al., 2012; Tazaz et al., 2013; Suda et
646 al., 2014). Isotope fractionation may also decrease under unlimited supply of substrates. For example,
647 Valentine et al. (2004) observed that the high partial pressure of H_2 decreased fractionation between
648 CO_2 and CH_4. They suggest that this could be due to limited reversibility of methanogenesis at excess
649 H_2. High partial pressure of H_2 may also inhibit some methanogenic species (Thauer et al., 2008), thus
650 changing the reaction pathway or even limiting it to abiotic. A combination of limited carbon supply

with excess H_2 could explain the high $\delta^{13}C_{CH4}$ values especially below 2300 m depth at Outokumpu and at Pyhäsalmi.

5.4 Carbon in the system CH_4-C_2H_6-C_3H_8

Even though some subsurface microorganisms may be capable of producing longer chained hydrocarbons (e.g. Taylor et al., 2000; Hinrichs et al., 2006), the vast majority of microbially generated hydrocarbon gas is CH_4, and the high CH_4/C_2+ ratio (>1000) is commonly used to separate microbial from thermogenic CH_4, even though lower ratios may also be observed due to preferential consumption (oxidation) or escape (diffusive or advective migration) of CH_4 (Bernard et al., 1976; Printzhofer and Huc, 1995; Whiticar, 1999). Figure 9 shows the classification of CH_4 into microbial and thermogenic based on the CH_4/C_2+ ratio in combination with the isotopic composition of CH_4, i.e. the classical Bernard diagram for the samples from the Fennoscandian Shield (Table EA2). In addition, potential limits are suggested for abiotic CH_4 in Fig. 9 which are based on data from the Zambales ophiolite (ZO) and mid-ocean ridges (MOR) (Horita and Berndt, 1999 and references therein), and artificial CH_4 from bit-metamorphism (Faber et al., 1999). If, instead, previous data from the Precambrian Shields with $\delta^{13}C_{CH4}$ values down to -50‰ VPDB are considered abiotic (cf. Fig. 2 and Sherwood Lollar et al. 1993b), the abiotic field would essentially include the whole thermogenic field.

The CH_4/C_2+ ratio is not capable of distinguishing abiotic hydrocarbons from microbial and thermogenic very well because the former can have both high and low ratios (Faber et al., 1999; Horita and Berndt, 1999; Tassi et al., 2012). For example, hydrocarbons produced by clay catalysed reactions differ from those of FTT synthesis, as they contain more aromatic compounds, instead of the dominance of linear alkanes typical for FTT, while the organosulphur pathway lacks alkane and alkene products (McCollom, 2013). Longer chained alkanes are also more probably produced in gaseous than aqueous systems (Lewan and Roy, 2011). When associated with extremely ^2H-poor and ^{13}C-rich CH_4, high concentrations of both H_2 and unsaturated hydrocarbons, the high CH_4/C_2+ ratio may indicate artificial CH_4 formed (from organic compounds often added in the drilling fluid) by bit-metamorphism (Faber et al., 1999). In this light, different formation processes can explain the different CH_4/C_2+ ratios of similarly ^{13}C enriched CH_4 at Outokumpu and Pyhäsalmi.

A further indication of different formation mechanisms comes from the comparison of $\delta^{13}C$ compositions of the alkanes (Fig. 3). The typical V-shaped pattern at Outokumpu is similar to that reported by Sherwood Lollar et al. (2008) from the Kidd Creek mine and four other sites in Precambrian shields in Canada and South Africa which they explained by abiotic polymerisation of hydrocarbons. In their model, the first step ($CH_4 \rightarrow C_2H_6$) is associated with isotope depletion but the fractionation then diminishes due to rapid polymerisation and is thereafter only controlled by isotope mass balance which leads to slight enrichment of ^{13}C from C_2H_6 onwards (Sherwood Lollar et al., 2008). The initial step of hydrocarbon generation by this mechanism could not be experimentally reproduced (McCollom et al., 2010) and the actual mechanism still remains elusive. Low (or decreasing) temperature might be a prerequisite for the preservation of such pattern as the polymerised hydrocarbons cannot split, and may explain why this trend is more common in nature than in experiments which have usually been performed at increasing temperatures (Zhang et al., 2013). Reversal of the carbon isotope trend may also be formed at the latest stages of thermogenic gas formation after the formation of longer chained hydrocarbons has ceased, allowing Rayleigh-type fractionation of carbon isotope composition of C_2H_6 and C_3H_8 to occur (Burruss and Laughrey 2010), Thus it may indicate shift from thermogenic to abiotic processes at environments where refractory organic carbon sources are present.

At Pyhäsalmi C_2H_6 is depleted in ^{12}C compared to CH_4 (Fig. 3), a trend that has been commonly associated with thermogenic hydrocarbons in which it forms as the result of break-up of organic molecules with increasing temperature (e.g. Sherwood Lollar et al., 2002; Zhang et al., 2013). The isotopic compositions are, however, much more ^{13}C enriched than in conventional thermogenic hydrocarbon occurrences and it is also difficult to find a plausible source for such gas in metavolcanic rocks.

5.5 Evidence for microbial methane

Methanogenic microorganisms have been found from both Outokumpu and Pyhäsalmi (e.g. Itävaara et al., 2011; Purkamo et al. 2015a, 2015b; Miettinen et al., 2015). Among the other sites within the Fennoscandian Shield, where isotopic data of CH_4 are available (Fig. 1), methanogens have been found also from Olkiluoto (Pedersen et al., 2008; Nyyssönen et al., 2012; Bomberg et al., 2014), but not from

Gravberg (Szewzyk et al. 1994), Hästholmen, Kivetty or Romuvaara (Haveman et al., 1999). To our knowledge, the other sites depicted in Fig. 1 have not been studied for their microbiology.

Methanotrophs, which oxidize CH_4 for living, also commonly accompany methanogens in deep crystalline rock environments (Nyyssönen et al., 2012; Purkamo et al., 2015a; Bomberg et al., 2015). However, methanogens and methanotrophs typically form only a marginal group of the microbial communities studied (e.g. Miettinen et al., 2015; Purkamo et al. 2015a, 2015b; Simkus et al., 2016). In contrast to previous views which suggest that the deep biosphere is dominated by autotrophs, Purkamo et al. (2015a) hypothesised that the biological deep carbon cycling in Outokumpu is mainly evoked by heterotrophic bacteria. The role of methanogens and methanotrophs in providing carbon for the whole community may however be more important than suggested by their relative proportion (Simkus et al., 2016).

In the Outokumpu Deep Drill Hole groundwater, methanogenic activity is both more common and more versatile at shallower depths above 1 km compared to the deeper levels (Purkamo et al., 2015a, 2015b). Purkamo et al. (2015b) retrieved methanogen communities from the DNA extracted from the fracture fluids of 180, 500, 2260 and 2300 m depths but only the samples from 500 and 967 m contained methanogen RNA. As RNA is used as a proxy for metabolically active species, this may indicate that the active microbial methanogenesis is restricted to the upper 1 km of the drill hole, or the deep dwelling methanogenic species cannot be detected with the methods used. Likewise, methanotrophy is more common at shallower depths not only at Outokumpu where methanotrophic communities have been found at 600, 900 and 1500 m depths but not from deeper levels (Purkamo et al. 2015a) but also in other sites within the Fennoscandian Shield (Kietäväinen and Purkamo, 2015).

Methanogenic species also vary with depth. At Outokumpu, aceticlastic (heterotrophic) *Methanosarcinales* prevail in the upper part of the drill hole and hydrogenotrophic (autotrophic) *Methanobacteriales* below 1300 m (Nyyssönen et al., 2014; Purkamo et al., 2015a). At Pyhäsalmi *Methanobacteriales* was the most common archaeal order found by DNA and RNA sequencing methods, although in the drill hole R-2247 *Thermoplasmata*, some of which also belong to methanogens, were dominating the archaeal RNA fraction (Miettinen et al., 2015). Indeed a general trend can be detected worldwide within the Precambrian shields that methanogens are more

metabolically diverse at shallower depths (Kietäväinen and Purkamo, 2015). Isotopic compositions of CH_4 among the Fennoscandian Shield sites also show that $\delta^{13}C_{CH4}$ values below -40‰ are exclusively found in the upper 1 km depth while values heavier than -20‰ appear to be more common at depths greater than 1.5 km (Fig. 10). At some extent this can be due to biased data as samples below 1.5 km are from only three sites (Outokumpu Deep Drill Hole, Pyhäsalmi and Gravberg) and from depths which mainly represent volcanic and igneous rocks. However, similar results have been recently obtained in the Witwatersrand basin in South Africa (Simkus et al., 2016).

5.6 Evidence for lithological control on the amount and isotopic composition of methane

Within the Fennoscandian Shield sites the depth dependence of CH_4/C_2+ ratio (Fig. 11) is poor. Instead the variation in CH_4/C_2+ seems to vary from site to site, which may indicate lithological control on the production of hydrocarbons. Previous observations from around the world suggest that in general hydrocarbons in igneous rocks have low CH_4/C_2+ ratios (<100), such as those at Pyhäsalmi, while higher ratios, similar to those at Outokumpu, have been found in the Zambales ophiolite and sediment covered ridges and even higher values (>1000) in the sediment free mid-ocean ridges (Fig. 9; Horita and Berndt, 1999; Tassi et al., 2012 and references therein). The differences may be related to availability of organic carbon sources or microbial activity, but may also arise from the differences in the abiotic formation mechanism and temperature/or pressure (see also discussion in 5.4).

Within the occurrences of crustal CH_4 in the Fennoscandian Shield (Fig. 1), the most ^{13}C depleted values are from Enonkoski (Sherwood Lollar et al., 1993a), Muhos and Tyrnävä (Heikkinen, 1972) (Fig. 10). The last two sites also drastically differ in their lithology from the other sites. They are located within glacial sediments on top of a 1300 Ma, non-metamorphosed sedimentary rocks (shale). These represent typical microbial CH_4 formed at low temperatures from abundant organic rich matter. Shallow (< 300 m) groundwater within non-metamorphosed sandstone of Pori also contains low amounts of relatively ^{12}C-rich CH_4 (Sherwood Lollar et al., 1993a).

The other sites have suffered from high temperature, meaning that preferable escape of lighter isotope has likely taken place leaving the remaining refractory organic remains depleted in ^{12}C (in the case of organic rich metasediments) or ^{12}C rich carbon perhaps never existed (in the case of magmatic rocks).

775 At Olkiluoto a hydraulically dynamic upper layer of around 200 m thick occurs (e.g. Pitkänen and
776 Partamies, 2007) which could provide microbes with abundant carbon and explain the sporadic
777 discoveries of ^{12}C rich CH_4. However the ^{12}C-rich CH_4 at Enonkoski, interpreted by Sherwood Lollar
778 et al. (1993a) to represent microbial CH_4, is more enigmatic and the other sites with confirmed
779 methanogenic activity do not generally show similar isotopic compositions together with C_2+ enriched
780 composition of the gas (Fig. 9).
781
782 Deep levels of the Pyhäsalmi mine are an example of magmatic rock environment where most of the
783 CH_4 has likely formed at high temperature, and possible artificial, abiotic synthesis. In addition to CH_4
784 such synthesis has also produced higher amounts of C_2+ compounds (Fig. 9), but resulted in overall
785 low potential of hydrocarbon generation, and thus low concentrations of hydrocarbons and, opposed to
786 abiotic low temperature hydrocarbons, may be characterised by ^{13}C enrichment with the increasing
787 chain length. In this same group belong Hästholmen (Haveman et al., 1999) and Gravberg (Jeffrey and
788 Kaplan, 1988) sites which are both located in granitic rocks and Romuvaara where the bedrock consists
789 of tonalite gneiss (Haveman et al., 1999). Slightly more ^{12}C-rich CH_4 is found from groundwater within
790 granitic surroundings of Kivetty (Haveman et al., 1999) and serpentinite and gabbro of Ylivieska
791 (Sherwood Lollar et al., 1993a). Except Ylivieska, with the maximum of 8.5 mmol l^{-1} CH_4 (Sherwood
792 Lollar et al., 1993a), the concentrations of CH_4 remain well below 1 mmol l^{-1} at these sites (Table
793 EA2).
794
795 In contrast to volcanic and granitic rocks, sites within metasedimentary rocks including the Outokumpu
796 Deep Drill Hole, Juuka, Olkiluoto, Vammala, Kotalahti and Sukkulansalo typically contain abundant
797 CH_4 (Fig. 1, Table EA2) and have CH_4/C_2+ ratios generally > 100. The close relatedness of
798 metasedimentary rocks, graphite rich black schists in particular, and the highest concentrations of CH_4
799 and high CH_4/C_2+ ratios together with $\delta^{13}C_{CH4}$ usually between -40 and -20 ‰ VPDB strongly support
800 the hypothesis that within the Fennoscandian Shield CH_4 is more commonly produced at low
801 temperatures by microbial methanogenesis and/or abiotic reactions from ancient organic compounds
802 (possibly through inorganic intermediates such as graphite) rather than at high temperature abiotic or
803 thermogenic processes.
804
805 **6. CONCLUSIONS**

Our observations suggest that there is a lithological and microbiological control on the abundance and isotopic composition of CH_4 in deep bedrock environments. Differences are related to the availability of carbon and hydrogen sources as well as processes behind the incorporation of hydrogen and carbon via abiotic and biotic pathways into hydrocarbon molecules. Supported by the whole data set available from the Fennoscandian Shield, which shows that CH_4 is much more abundant in metasedimentary rocks than in magmatic rocks and exceptionally high if graphitic rocks are around, the carbon source for CH_4 formation is suggested to be mainly organic in origin. Rather than being thermogenic relic, crustal CH_4 within the Fennoscandian Shield is more likely produced at low temperatures from ancient organic compounds by microbial methanogenesis or abiotically through inorganic intermediates such as graphite. These crustal gases are characterized by the lack of major amounts of C_2+ hydrocarbons and ^{13}C rich CH_4. Microbiological together with isotope geochemical evidence suggest that microbial methanogenesis and thus microbial CH_4 is more common at depths shallower than 1.5 km. Minor amounts of CH_4, especially in magmatic rock settings and greater depths, has likely formed at high temperature abiotic synthesis which has also produced higher proportions of C_2+ compounds, but resulted in overall lower potential of hydrocarbon generation, and thus lower concentrations of hydrocarbons.

ACKNOWLEDGEMENTS

We want to thank Satu Vuoriainen for cutting the fracture mineral samples, Arja Henttinen for the preparation of vials for DIC sampling and Arto Pullinen for assisting in the field. Bo Johanson helped with the SEM analyses. Elina Sahlstedt advised in the isotopic analyses of calcites. The Pyhäsalmi Mine (First Quantum Minerals) is thanked for the possibility to take samples in the mine; especially the help of Mikko Numminen and Toni Leskinen was indispensable. Lotta Purkamo provided valuable comments on the manuscript. Taru Toppi and Juha Karhu also contributed to this study. Randy Stotler, Tom Darrah and an anonymous Reviewer are thanked for their helpful comments on the manuscript. This study was funded by the Academy of Finland (Deep Life: Grant 133348/2009), the Finnish Research Program on Nuclear Waste Management (KYT2014 and KYT2018 grants to projects SALAMI and RENGAS, respectively) and Geological Survey of Finland. HN was supported by the Academy of Finland awarded Academy Fellow post (project 136455).

837

838 **REFERENCES**

839

840 Ahonen L., Kietäväinen R., Kortelainen N., Kukkonen I. T., Pullinen A., Toppi T., Bomberg M.,
841 Itävaara M., Nousiainen A., Nyyssönen M. and Öster M. (2011) Hydrogeological characteristics of the
842 Outokumpu Deep Drill Hole. *Geol. Surv. Finl., Spec. Paper* **51**, 151-168.

843

844 Anderson R.B. (1984) *The Fischer-Tropsch synthesis*. Academic Press, New York.

845

846 Atekwana E. A. and Krishnamurthy R. V. (1998) Seasonal variations of dissolved inorganic carbon and
847 $\delta^{13}C$ of surface waters: application of a modified gas evolution technique. *J. Hydrol.* **205**, 265-278.

848

849 Balabane M., Galimov E., Hermann M. and Létolle R. (1987) Hydrogen and carbon isotope
850 fractionation during experimental production of bacterial methane. *Org. Geochem.* **11**, 115-119.

851

852 Bernard B.B., Brooks J.M. and Sackett W.M (1976) Natural gas seepage in the Gulf of Mexico. *Earth*
853 *Planet. Sci. Lett.* **31**, 48-54.

854

855 Blyth A.R., Frape S.K. and Tullborg E.-L. (2009) A review and comparison of fracture mineral
856 investigations and their application to radioactive waste disposal. *Appl. Geochem.* **24**, 821-835.

857

858 Bomberg M., Nyyssönen M., Pitkänen P., Lehtinen A. and Itävaara M. (2015) Active microbial
859 communities inhabit sulphate-methane interphase in deep bedrock fracture fluids in Olkiluoto, Finland
860 *BioMed Res. Int.* Article ID 979530, doi: 10.1155/2015/979530

861

862 Bomberg M., Nyyssönen M., Nousiainen A., Hultman J., Paulin L., Auvinen P. and Itävaara, M. (2014)
863 Evaluation of molecular techniques in characterization of deep terrestrial biosphere. *Open J. Ecol.* **4**,
864 468-487.

865

866 Bottinga Y. (1969) calculated fractionation factors for carbon and hydrogen isotope exchange in the
867 system calcite-carbon dioxide-graphite-methane-hydrogen-water vapour. *Geochim. Cosmochim. Acta*
868 **33**, 49-64.
869
870 Bradley A.S., Hayes J.M. and Summons R.E. (2009) Extraordinary ^{13}C enrichment of diether lipids at
871 the Lost City Hydrothermal Field indicates a carbon-limited ecosystem. *Geochim. Cosmochim. Acta*
872 **73**, 102-118.
873
874 Burke R. A., Jr. (1993) Possible influence of hydrogen concentration on microbial methane stable
875 hydrogen isotopic composition. *Chemosphere* **26**, 55-67.
876
877 Burruss R.C. and Laughrey C.D. (2010) Carbon and hydrogen isotopic reversals in deep basin gas:
878 Evidence for limits to the stability of hydrocarbons. *Org. Geochem.* **41**, 1285-1296.
879
880 Claesson S., Huhma H., Kinny P. D. and Williams I. S. (1993) Svecofennian detrital zircon ages –
881 implications for the Precambrian evolution of the Baltic Shield. *Precambrian Res.* **64**, 109-130.
882
883 Clark I. and Fritz P. (1997) *Environmental isotopes in hydrogeology*. Lewis Publishers, Boca Raton.
884
885 Darrah T.H., Vengosh A., Jackson R.B., Warner N.R. and Poreda R.J. (2014) Noble gases identify the
886 mechanisms of fugitive gas contamination in drinking water wells overlying the Marcellus and Barnett
887 Shales. *PNAS* **111**, 14076-14081.
888
889 Devirts A.L., Gagauz F.G., Grinenko V.A., Lagutina Ye.P., Pereverzov V.V. and Shukolyukov Yu.A.
890 (1993) Origin of hydrogen in Kempirsay-intrusion ultramafites. *Geochem. Internat.* **30**, 139-144.
891
892 Drake H., Åström M., Heim C., Broman C., Åström J., Whitehouse M., Ivarsson M., Siljeström S. and
893 Sjövall P. (2015) Extreme ^{13}C depletion of carbonates formed during oxidation of biogenic methane in
894 fractured granite. *Nat. Commun.* **6**, 7020, doi:10.1038/ncomms8020
895

896 Duan Z. and Li D. (2008) Coupled phase and aqueous species equilibrium of the H_2O– CO_2–NaCl–
897 $CaCO_3$ system from 0° to 250°C, 1 to 1000 bar with NaCl concentrations up to saturation of halite.
898 *Geochim. Cosmochim. Acta* **72**, 5128-5145.
899
900 Etiope G. and Schoell M. (2014) Abiotic gas: atypical, but not rare. *Elements* **10**, 291-296.
901
902 Etiope, G. and Sherwood Lollar B. (2013) Abiotic methane on Earth. *Rev. Geophys.* **51**, 276-299.
903
904 Etiope G., Baciu C.L. and Schoell M. (2011) Extreme methane deuterium, nitrogen and helium
905 enrichment in natural gas from the Homorod seep (Romania). *Chem. Geol.* **280**, 89-96.
906
907 Etiope G., Ehlmann B.L. and Schoell M. (2013) Low temperature production and exhalation of
908 methane from serpentinized rocks on Earth: A potential analog for methane production on Mars. *Icarus*
909 **224**, 276-285.
910
911 Faber E., Whiticar M.J. and Gerling P. (1999) Comparison of hydrocarbons from unconventional
912 sources: KTB, EPR and bit metamorphism. *Geol. Jb.* **D107**, 175-194.
913
914 Fuex A.N. (1980) Experimental evidence against an appreciable isotopic fractionation of methane
915 during migration. Phys. Chem. Earth 12, 725-732.
916
917 Giggenbach W.F. (1982) Carbon-13 exchange between CO_2 and CH_4 under geothermal conditions.
918 *Geochim. Cosmochim. Acta* **46**, 159-165.
919
920 Haveman S.A., Pedersen K. and Ruotsalainen P. (1999) Distribution and metabolic diversity of
921 microorganisms in deep igneous rock aquifers of Finland. *Geomicrobiol. J.* **16**, 277-294.
922
923 Heikkinen A. (1972) Tyrnävän ja Muhoksen maakaasuista. *Geologi* **24**, 73-76. (In Finnish with an
924 English summary).
925

926 Heikkinen N. (2016) Kaasujen liukoisuus Outokummun syväkairareiän suolaisessa pohjavedessä. MSc
927 Thesis, University of Helsinki, 77 p. (In Finnish with an English abstract "Solubility of gases in saline
928 waters of the Outokumpu Deep Drill Hole", available on-line:
929 https://helda.helsinki.fi/bitstream/handle/10138/159367/Heikkinen_gradu.pdf?sequence=3)
930
931 Hinrichs K.-U., Hayes J.M., Bach W., Spivack A.J., Hmelo L.R., Holm N.G., Jonson C.G. and Sylva
932 S.P. (2006) Biological formation of ethane and propane in the deep marine subsurface. *PNAS* **103**,
933 14684-14689.
934
935 Horibe Y. and Craig H. (1995) D/H fractionation in the system methane-hydrogen-water. *Geochim.*
936 *Cosmochim. Acta* **59**, 5209-5217.
937
938 Horita J. and Berndt M.E. (1999) Abiogenic methane formation and isotopic fractionation under
939 hydrothermal conditions. *Science* **285**, 1055-1057.
940
941 Hyyppä J. (1981) Geologisten erityisolosuhteiden vaikutus pohjaveden laatuun. *Vesihallituksen*
942 *monistesarja* **91**, 117-130 (In Finnish).
943
944 Itävaara M., Nyyssönen M., Kapanen A., Nousiainen A., Ahonen L. and Kukkonen I. (2011)
945 Characterization of bacterial diversity to a depth of 1500 m in the Outokumpu deep borehole,
946 Fennoscandian Shield. *FEMS Microbiol. Ecol.* **77**, 295-309.
947
948 Jacquemin M., Beuls A. and Ruiz P. (2010) Catalytic production of methane from CO_2 and H_2 at low
949 temperature: Insight on the reaction mechanism. *Catal. Today* **157**, 462-366.
950
951 Jeffrey A.W.A. and Kaplan I.R. (1988) Hydrocarbons and inorganic gases in the Gravberg-1 well,
952 Siljan Ring, Sweden. *Chem. Geol.* **71**, 237-255.
953
954 Jenden P.D., Kaplan I.R., Poreda R.J. and Craig H. (1988) Origin of nitrogen-rich natural gases in the
955 California Great Valley: Evidence from helium, carbon and nitrogen isotope ratios. *Geochim.*
956 *Cosmochim. Acta* **52**, 851-861.

957
958 Karhu J.A. (1993) Paleoproterozoic evolution of the carbon isotope ratios of sedimentary carbonates in
959 the Fennoscandian Shield. *Geol. Surv. Finl., Bull.* **371**, 87 p.
960
961 Kay C.M., Haanela A. and Jonson D.B. (2014) Microorganisms in subterranean acidic waters within
962 Europe's deepest metal mine. *Res. Microbiol.* **165**, 705-712.
963
964 Kelley C.A., Poole J.A., Tazaz A.M., Chanton J.P. and Bebout B.M. (2012) Substrate limitation for
965 methanogenesis in hypersaline environments. *Astrobiology* **12**, 89-97.
966
967 Kietäväinen R. and Purkamo L. (2015) The origin, source and cycling of methane in deep crystalline
968 rock biosphere. *Front. Microbiol.* **6**, 725, doi: 10.3389/fmicb.2015.00725
969
970 Kietäväinen R., Ahonen L., Kukkonen I. T., Hendriksson N., Nyyssönen M. and Itävaara M. (2013)
971 Characterisation and isotopic evolution of saline waters of the Outokumpu Deep Drill Hole, Finland –
972 Implications for water origin and deep terrestrial biosphere. *Appl. Geochem.* **32**, 37-51.
973
974 Kietäväinen R., Ahonen L., Kukkonen I.T., Niedermann S. and Wiersberg T. (2014) Noble gas
975 residence times of saline waters within crystalline bedrock, Outokumpu Deep Drill Hole, Finland.
976 *Geochim. Cosmochim. Acta* **145**, 159-174.
977
978 Koistinen T., Stephens M.B., Bogatchev V., Nordgulen Ø., Wennerström M. and Korhonen J. (comp.)
979 (2001) Geological map of the Fennoscandian Shield, scale 1:2 000 000. Trondheim: Geological Survey
980 of Norway, Uppsala: Geological Survey of Sweden, Moscow: Ministry of Natural Resources of Russia,
981 Espoo: Geological Survey of Finland.
982
983 Kontinen A., Peltonen P. and Huhma H. (2006) Description and genetic modelling of the Outokumpu-
984 type rock assemblage and associated sulphide deposits. GTK report M 10.4 /2006/1 (Available online:
985 http://arkisto.gtk.fi/m10/m10_4_2006_1.pdf).
986

Kotelnikova S. (2002) Microbial production and oxidation of methane in deep subsurface. *Earth-Sci. Rev.* **58**, 367-395.

Kousa J., Marttila E. and Vaasjoki M. (1994) Petrology, geochemistry and dating of Paleoproterozoic metavolcanic rocks in the Pyhäjärvi area, central Finland. *Geol. Surv. Finl., Spec. Paper* **19**, 7-27.

Kukkonen I.T., Rath V., Kivekäs L., Šafanda J. and Čermák V. (2011) Geothermal studies of the Outokumpu Deep Drill Hole, Finland: vertical variation in heat flow and palaeoclimatic implications. *Phys. Earth Planet. Inter.* **188**, 9-25.

Lahtinen R., Huhma H., Kontinen A., Kohonen J. and Sorjonen-Ward P. (2010) New constraints for the source characteristics, deposition and age of the 2.1-1.9 Ga metasedimentary cover at the western margin of the Karelian Province. *Precambrian Res.* **176**, 77-93.

Lécluse C. and Robert F. (1994) Hydrogen isotope exchange reaction rates: Origin of water in the inner solar system. *Geochim. Cosmochim. Acta* **58**, 2927-2939.

Lewan M.D. and Roy S. (2011) Role of water in hydrocarbon generation from Type-I kerogen in Mahogany oil shale of the Green River Formation. Organic Geochemistry **42**, 31-41.

Lin L.-H., Hall J., Lippmann-Pipke J., Ward J.A., Sherwood Lollar B., DeFlaun M., Rothmel R., Moser D., Gihring T.M., Mislowack B. and Onstott T.C. (2005a) Radiolytic H_2 in continental crust: Nuclear power for deep subsurface microbial communities. *Geochem., Geophys., Geosyst.* **6**, Q07003, doi:10.1029/2004GC000907.

Lin L.-H., Slater G.F., Sherwood Lollar B., Lacrampe-Couloume G. and Onstott T.C., (2005b) The yield and isotopic composition of radiolytic H_2, a potential energy source for the deep subsurface biosphere. *Geochim. Cosmochim. Acta* **69**, 893-903.

Loukola-Ruskeeniemi K. (1999) Origin of black shales and the serpentinite-associated Cu-Zn-Co ores at Outokumpu, Finland. *Econ. Geol.* **94**, 1007-1028.

Lyon G.L. and Hulston J.R. (1984) Carbon and hydrogen isotopic compositions of New Zealand geothermal gases. *Geochim. Cosmochim. Acta* **48**, 1161-1171.

McCollom T.M. (2013) Laboratory simulations of abiotic hydrocarbon formation in Earth's deep subsurface. *Rev. Mineral. Geochem.* **75**, 467-494.

McCollom T.M. and Bach W. (2009) Thermodynamic constraints on hydrogen generation during serpentinization of ultramafic rocks. *Geochim. Cosmochim. Acta* **73**, 856-875.

McCollom T.M., Sherwood Lollar B.S., Lacrampe-Couloume G. and Seewald J.S. (2010) The influence of carbon source on abiotic organic synthesis and carbon isotope fractionation under hydrothermal conditions. *Geochim. Cosmochim. Acta* **74**, 2717-2740.

Miettinen H., Kietäväinen R., Sohlberg E., Numminen M., Ahonen L. and Itävaara M. (2015) Microbiome composition and geochemical characteristics of deep subsurface high-pressure environment, Pyhäsalmi mine Finland *Front. Microbiol.* **6**, 1203, doi: 10.3389/fmicb.2015.01203

Mischler J.A., Sowers T.A., Alley R.B., Battle M., McConnell J.R., Mitchell L., Popp T., Sofen E. and Spencer M.K. (2009) Carbon and hydrogen isotopic composition of methane over the last 1000 years. *Global Biogeochem. Cycles* **23**, GB4024, doi:10.1029/2009GB003460.

Mook W.G., Bommerson J.C. and Staverman W.H. (1974) Carbon isotope fractionation between dissolved bicarbonate and gaseous carbon dioxide. *Earth Planet. Sci. Lett.* **22**, 169-176.

Neubeck A., Thanh Duc N., Bastviken D., Crill P. and Holm N.G. (2011) Formation of H_2 and CH_4 by weathering of olivine at temperatures between 30 and 70ºC. *Geochem. Trans.* **12**:6.

Ni Y., Ma Q., Ellis G.S., Dai J., Katz B., Zhang S. and Tang Y. (2011) Fundamental studies on kinetic isotope effect (KIE) on hydrogen isotope fractionation in natural gas systems. *Geochim Cosmochim. Acta* **75**, 2696-2707.

Nurmi P.A. and Kukkonen I.T. (1986) A new technique for sampling water and gas from deep drill holes. *Can. J. Earth Sci.* **23**, 1450-1454.

Nyyssönen M., Bomberg M., Kapanen A., Nousiainen A., Pitkänen P. and Itävaara, M. (2012) Methanogenic and sulphate-reducing microbial communities in deep groundwater of crystalline rock fractures in Olkiluoto, Finland. *Geomicrobiol. J.* **29**, 863-878.

Nyyssönen M., Hultman J., Ahonen L., Kukkonen I., Paulin L., Laine P., Itävaara M. and Auvinen P. (2014) Taxonomically and functionally diverse microbial communities in deep crystalline rocks of the Fennoscandian shield. *ISME J.* **8**, 126-138.

O'Neil J.R., Clayton R.N. and Mayeda T.K. (1969) Oxygen isotope fractionation in divalent metal carbonates. *J. Chem. Phys.* **51**, 5547-5558.

Park A.F. (1988) Nature of the early Proterozoic Outokumpu assemblage, eastern Finland. *Precambrian Res.* **38**, 131-146.

Pedersen K., Ekendahl S., Tullborg E.-L., Furnes H., Thorseth I. and Tumyr O. (1997) Evidence of ancient life at 207 m depth in a granitic aquifer. *Geology* **25**, 827-830.

Pedersen K., Arlinger J., Eriksson S., Hallbeck A., Hallbeck L., and Johansson J. (2008). Numbers, biomass and cultivable diversity of microbial populations relate to depth and borehole-specific conditions in groundwater from depths of 4–450 m in Olkiluoto, Finland. *ISME J.* **2**, 760-775.

Peltonen P., Kontinen A., Huhma H. and Kuronen U. (2008) Outokumpu revisited: New mineral deposit model for the mantle peridotite-associated Cu-Co-Zn-Ni-Ag-Au sulphide deposits. *Ore Geol. Rev.* **33**, 559-617.

1078 Pitkänen P. and Partamies S. (2007) Origin and implications of dissolved gases in groundwater at
1079 Olkiluoto. Posiva report 2007-04, Posiva Oy, Olkiluoto (Available online:
1080 http://www.posiva.fi/files/341/Posiva2007-04web.pdf).
1081
1082 Prinzhofer A.A. and Huc A.Y. (1995) Genetic and post-genetic molecular and isotopic fractionations in
1083 natural gases. *Chem. Geol.* **126**, 281-290.
1084
1085 Purkamo L., Bomberg M., Nyyssönen, M., Kukkonen I., Ahonen L., Kietäväinen R. and Itävaara M.
1086 (2013) Dissecting the deep biosphere: retrieving authentic microbial communities from packer-isolated
1087 deep crystalline bedrock fracture zones. *FEMS Microbiol. Ecol.* **85**, 324-337.
1088
1089 Purkamo L., Bomberg M., Nyyssönen M., Kukkonen I., Ahonen L. and Itävaara M. (2015a)
1090 Heterotrophic communities supplied by ancient organic carbon predominate in deep Fennoscandian
1091 bedrock fluids. *Microb. Ecol.* **69**, 319-332.
1092
1093 Purkamo L., Bomberg M., Kietäväinen R., Salavirta H., Nyyssönen M., Nuppunen-Puputti M., Ahonen
1094 L., Kukkonen I. and Itävaara M. (2015b) The keystone species of Precambrian deep bedrock biosphere
1095 belong to *Burkholderiales* and *Clostridiales*. *Biogeosciences Discuss.* **12**, 18103-18150, doi:
1096 10.5194/bgd-12-18103-2015
1097
1098 Rajala P., Bomberg M. Kietäväinen R., Kukkonen I., Ahonen L., Nyyssönen M. and Itävaara M. (2015)
1099 Rapid reactivation of deep subsurface microbes in the presence of C-1 compounds. *Microorganisms* **3**,
1100 17-33.
1101
1102 Reeves E.P., Seewald J.S. and Sylva S.P. (2012) Hydrogen isotope exchange between *n*-alkanes and
1103 water under hydrothermal conditions. *Geochim. Cosmochim. Acta* **77**, 582-599.
1104
1105 Regenspurg S., Wiersberg T., Brandt W., Huenges E., Saadat A., Schmidt K. and Zimmermann G.
1106 (2010) Geochemical properties of saline geothermal fluids from the in-situ geothermal laboratory Groß
1107 Schönebeck (Germany). *Chem. Erde* **70**, 3-12.
1108

1109 Romanek C.S., Zhang C.L., Li Y., Horita J., Vali H., Cole D.R. and Phelps T.J. (2003) Carbon and
1110 hydrogen isotope fractionations associated with dissimilatory iron-reducing bacteria. *Chem. Geol.* **195**,
1111 5-16.
1112
1113 Sahlstedt E., Karhu J.A., Pitkänen P. and Whitehouse M. (2016) Biogenic processes in crystalline
1114 bedrock fractures indicated by carbon isotope signatures of secondary calcite *Appl. Geochem.* **67**, 30-
1115 41.
1116
1117 Salomons W. and Mook W.G. (1986) Isotope geochemistry of carbonates in the weathering zone. In
1118 *Handbook of environmental isotope geochemistry*, Vol. 1, The terrestrial environment (eds. Fritz, P.
1119 and Fontes J.C.). Elsevier, Amsterdam pp. 239-270.
1120
1121 Säntti J., Kontinen A., Sorjonen-Ward P., Johanson B. and Pakkanen L. (2006) Metamorphism and
1122 chromite in serpentinized and carbonate-silica-altered peridotites of the Paleoproterozoic Outokumpu-
1123 Jormua Ophiolite Belt, eastern Finland. *Int. Geol. Rev.* **48**, 494-546.
1124
1125 Schloemer S. and Krooss B.M. (2004) Molecular transport of methane, ethane and nitrogen and the
1126 influence of diffusion on the chemical and isotopic composition of natural gas accumulations.
1127 *Geofluids* **4**, 81-108.
1128
1129 Schrenk M.O., Brazelton W.J. and Lang S.Q. (2013) Serpentinization, carbon, and deep life. *Rev.*
1130 *Mineral. Geochem.* **75**, 575-606.
1131
1132 Schoell M. (1980) The hydrogen and carbon isotopic composition of methane from natural gases of
1133 various origins. *Geochim. Cosmochim. Acta* **44**, 649-661.
1134
1135 Schoell M. (1983) Isotope techniques for tracing migration of gases in sedimentary basins. *J. Geol.*
1136 *Soc. London* **140**, 415-422.
1137
1138 Schoell M. (1988) Multiple origins of methane in the Earth. *Chem. Geol.* **71**, 1-10.
1139

1140 Sephton M.A. and Hazen R.M. (2013) On the origins of deep hydrocarbons. *Rev. Mineral. Geochem.*
1141 **75**, 449-465.
1142
1143 Sherwood B., Fritz P., Frape S.K., Macko S.A., Weise S.M. and Welhan J.A. (1988) Methane
1144 occurrences in the Canadian Shield. *Chem. Geol.* **71**, 223-236.
1145
1146 Sherwood Lollar B., Frape S.K., Fritz P., Macko S.A., Welhan J.A., Blomqvist R. and Lahermo P.W.
1147 (1993a) Evidence for bacterially generated hydrocarbon gas in Canadian Shield and Fennoscandian
1148 Shield rocks. *Geochim. Cosmochim. Acta* **57**, 5073-5085.
1149
1150 Sherwood Lollar B., Frape S.K., Weise S.M., Fritz P., Macko S.A. and Welhan J.A. (1993b) Abiogenic
1151 methanogenesis in crystalline rocks. *Geochim. Cosmochim. Acta* **57**, 5087-5097.
1152
1153 Sherwood Lollar B., Westgate,T.D., Ward J.A., Slater G.F. and Lacrampe-Couloume G. (2002)
1154 Abiogenic formation of alkanes in the Earth's crust as a minor source for global hydrocarbon
1155 reservoirs. *Nature* **416**, 522-524.
1156
1157 Sherwood Lollar B., Lacrampe-Couloume G., Voglesonger K., Onstott T.C., Pratt L.M. and Slater G.F.
1158 (2008) Isotopic signatures of CH4 and higher hydrocarbon gases from Precambrian Shield sites: A
1159 model for abiogenic polymerization of hydrocarbons. *Geochim. Cosmochim. Acta* **72**, 4778-4795.
1160
1161 Simkus D.N., Slater G.F., Sherwood Lollar B., Wilkie K., Kieft T.L., Magnabosco C., Lau M.C.Y.,
1162 Pullin M.J., Hendrickson S.B., Wommack K.E., Sakowski E.G., van Heerden E., Kuloyo O., Linage
1163 B., Borgonie G. and Onstott T.C. (2016) Variations in microbial carbon sources and cycling in the deep
1164 continental subsurface. *Geochim. Cosmochim. Acta* **173**, 264-283.
1165
1166 Stotler R., Frape S.K., Ahonen L., Clark I., Greene S., Hobbs M., Johnson E., Lemieux J.-M., Peltier
1167 R., Pratt L., Ruskeeniemi T., Sudicky E. and Tarasov L. (2010) Origin and stability of a permafrost
1168 methane hydrate occurrence in the Canadian Shield. *Earth Planet. Sci. Lett.* **296**, 384-394.
1169

1170 Suda K., Ueno Y., Yoshizaki M., Nakamura H., Kurokawa K., Nishiyama E., Yoshino K., Hongoh Y.,
1171 Kawachi K., Omori S., Yamada K., Yoshida N. and Maruyama S. (2014) Origin of methane in
1172 serpentinite-hosted hydrothermal systems: The CH_4-H_2-H_2O hydrogen isotope systematic of the
1173 Hakuba Happo hot spring. *Earth Planet. Sci. Lett.* **386**, 112-125.
1174
1175 Sugimoto A. and Wada E. (1995) Hydrogen isotopic composition of bacterial methane:
1176 CO_2/H_2 reduction and acetate fermentation. *Geochim. Cosmochim. Acta* **59**, 1329-1337.
1177
1178 Szewzyk U., Szewzyk R. and Stenström T.-A. (1994) Thermophilic, anaerobic bacteria isolated from a
1179 deep borehole in granite in Sweden. *Proc. Natl. Acad. Sci.* **91**, 1810-1813.
1180
1181 Taran L.N., Onoshko M.P. and Mikhailov N.D. (2011) Structure and composition of organic matter
1182 and isotope geochemistry of the Palaeoproterozoic graphite and sulphide-rich metasedimetary rocks
1183 from the Outokumpu Deep Drill Hole, eastern Finland. *Geol. Surv. Finl., Spec. Paper* **51**, 219-228.
1184
1185 Taran Y.A., Klinger G.A. and Sevastianov V.S. (2007) Carbon isotope effects in the open-system
1186 Fischer-Tropsch synthesis. *Geochim. Cosmochim. Acta* **71**, 4474-4487.
1187
1188 Tassi F., Fiebig J., Vaselli O. and Nocentini M. (2012) Origins of methane discharging from volcanic-
1189 hydrothermal, geothermal and cold emissions in Italy. *Chem. Geol.* **310-311**, 36-48.
1190
1191 Taylor S.W., Sherwood Lollar B. and Wassenaar L.I. (2000) Bacteriogenic ethane in near-surface
1192 aquifers: Implications for leaking hydrocarbon well bores. *Environ. Sci. Technol.* **34**, 4727-4732.
1193
1194 Tazaz A.M., Bebout B.M., Kelley C.A., Poole J. and Chanton J.P. (2013) Redefining the isotopic
1195 boundaries of biogenic methane: Methane from endoevaporites. *Icarus* **224**, 268-275.
1196
1197 Thauer R.K., Kaster A., Seedorf H., Buckel W. and Hedderich R. (2008) Methanogenic archaea:
1198 ecologically relevant differences in energy conservation. *Nat. Rev. Microbiol.* **6**, 579-591.
1199

1200 Toppi T. (2010) Kallioperän kaasujen koostumus ja isotoopit Outokummun syväreiässä. M.Sc. thesis,
1201 Univ. Helsinki (in Finnish with an English abstract).
1202
1203 USGS (2014) *PHREEQC*. Computer codes, United States Geological Survey.
1204 (http://wwwbrr.cr.usgs.gov/projects/GWC_coupled/phreeqc/)
1205
1206 Valentine D. L., Chidthaisong A., Rice A., Reeburgh W.S. and Tyler S.C. (2004) Carbon and hydrogen
1207 isotope fractionation by moderately thermophilic methanogens. *Geochim. Cosmochim. Acta* **68**, 1571-
1208 1590.
1209
1210 Västi K. (2011) Petrology of the drill hole R2500 at Outokumpu, eastern Finland – the deepest drill
1211 hole ever drilled in Finland. *Geol. Surv. Finl., Spec. Paper* **51**, 17-46.
1212
1213 Vovk I.F. (1987) Radiolytic salt enrichment and brines in the crystalline basement of the East European
1214 Platform. Geol. Assoc. Canada Special Paper **22**, 197-210.
1215
1216 Wallin B. and Peterman Z. (1999) Calcite fracture fillings as indicators of paleohydrology at Laxemar
1217 at the Äspö Hard Rock Laboratory, southern Sweden. *Appl. Geochem.* **14**, 953-962.
1218
1219 Wang Y., Sessions A.L., Nielsen R.J. and Goddard III W.A. (2009) Equilibrium $^{2}H/^{1}H$ fractionations in
1220 organic molecules. II: Linear alkanes, alkenes, ketones, carboxylic acids, esters, alcohols and ethers.
1221 *Geochim. Cosmochim. Acta* **73**, 7076-7086.
1222
1223 Ward J., Slater G., Moser D., Lin L., Lacrampe-Couloume G., Bonin A., Davidson M., Hall J.A.,
1224 Mislowack B., Bellamy R.E.S., Onstott T.C. and Sherwood Lollar B. (2004) Microbial hydrocarbon
1225 gases in the Witwatersrand Basin, South Africa: implications for the deep biosphere. *Geochim.*
1226 *Cosmochim. Acta* **68**, 3239-3250.
1227
1228 Whiticar M. J. (1999) Carbon and hydrogen isotope systematic of bacterial formation and oxidation of
1229 methane. *Chem. Geol.* **161**, 291-314.
1230

1231 Zhang S., Mi J. and He K. (2013) Synthesis of hydrocarbon gases from four different carbon sources
1232 and hydrogen gas using a gold-tube system by Fischer-Tropsch method. *Chem. Geol.* **349-350**, 27-35.
1233
1234
1235
1236

Figure captions

Fig. 1. A simplified lithological map of the Fennoscandian Shield in Sweden and Finland showing the sites investigated for their isotopic composition of CH_4 in this study and Heikkinen (1972), Hyyppä (1981), Jeffrey and Kaplan (1988), Sherwood Lollar et al. (1993a, 1993b), Haveman et al. (1999) and Pitkänen and Partamies (2007). Detailed lithologies are given for the Pyhäsalmi mine and Outokumpu Deep Drill Hole sites: MV = mafic volcanite, T = tonalite, FV = felsic volcanite, MS = mica schist, BS = black schist, O = ophiolitic rocks, GR = granodiorite. Basemap redrawn after Koistinen et al. (2001).

Fig. 2. Genetic classification of the Outokumpu Deep Drill Hole and Pyhäsalmi mine CH_4 based on the H and C isotopic composition. Fields are according to Etiope et al. (2013), and are based on traditional classification of microbial and thermogenic gas (e.g. Schoell 1988) and additional data from various geological environments. The abiotic field is based on data from volcanic-hydrothermal environments (V), serpentinized systems (S) and previous data from Precambrian shields (P) (Etiope et al. 2013 and references therein). Within the thermogenic field "O" refers to CH_4 occurring with oil and "D" refers to dry gas. Isotopic composition of CH_4 in the atmosphere (Mischler et al., 2009) is marked with X. For Outokumpu the samples are coded according the sampling technique: small circles = pumped, large circles = PDS and PAVE, and + = tube sampling. Pyhäsalmi samples = diamonds.

Fig. 3. Plot of carbon isotope compositions of methane, ethane and propane versus carbon number. Most of the samples from Outokumpu show relative depletion of ^{13}C in C_2H_6 compared to CH_4 and few samples where isotopic composition of C_3H_8 was determined further reveal a V-shaped pattern. In contrast, two samples from Pyhäsalmi (R-2247) display increase in ^{13}C with increasing chain length.

Fig. 4. Carbon isotope compositions of different carbon containing phases along the Outokumpu Deep Drill Hole. Major zones of groundwater flow are shown with white and gray arrows which indicate flow into the bedrock and into the drill hole, respectively (Ahonen et al., 2011; Kietäväinen et al., 2013). Isotopic composition of graphite is from Taran et al. (2011).

Fig. 5. a) CH_4/N_2 ratio and b) N_2/Ar ratio versus depth at Outokumpu and $\delta^{13}C_{CH4}$ versus c) CH_4/N_2 and d) N_2/Ar at Outokumpu and Pyhäsalmi. All ratios have been corrected for air-contamination by assuming that the concentration of oxygen in indigenous fracture fluids is zero (Kietäväinen et al. 2014). Symbols as in Fig. 2. In a) and b) different water types described by Kietäväinen et al. (2013) on the basis of water stable isotopes and dissolved solids, are indicated with roman numerals and appear to correspond with different gas types. Fluctuation in the relative gas compositions during pumping likely reflects bubble formation (differences in solubility) and/or heterogeneous gas source. In c) and d) changes in the x-y space may occur due to oxidation (increase in $\delta^{13}C_{CH4}$ and decrease in CH_4/N_2 ratio), methanogenesis (decrease in $\delta^{13}C_{CH4}$ and increase in CH_4/N_2 ratio), diffusion (decrease in $\delta^{13}C_{CH4}$, decrease in CH_4/N_2 and increase in the N_2/Ar ratio in the diffused gas), and mixing (linear change in the case of two component mixing). Although few samples (1820 m pumped, Pyhäsalmi R-2227) may have been affected by oxidation, most of the variation can be explained by mixing between gases emanating from different fracture zones.

Fig. 6. Hydrogen isotope concordance diagrams for the system CH_4-H_2O-H_2, based on equations for a) CH_4-H_2 and H_2O-H_2 and b) CH_4-H_2O and H_2-H_2O isotope equilibrium from Horibe and Craig (1995). Samples from the Outokumpu Deep Drill Hole (circles) and Pyhäsalmi mine drill hole R-2247 (diamonds) show equilibration temperatures below 50ºC and 100ºC, respectively.

Fig. 7. Isotopic fractionation of hydrogen between H_2O and CH_4. Equilibrium fractionation (Horibe and Craig 1995) is shown as broken lines for three different temperatures relevant for *in situ* conditions at the Outokumpu Deep Drill Hole and Pyhäsalmi mine. Characteristic fractionation related to microbial CO_2 reduction (C) and acetate fermentation (A) were calculated according to Whiticar (1999) with a maximum isotope offset for the acetate fermentation of -370‰ (lines) and Sugimoto and Wada (1995) (dotted lines). Symbols as in Fig. 2.

Fig. 8. a) Carbon and b) oxygen isotope compositions of calcites along the Outokumpu Deep Drill Hole. Isotopic equilibrium at ambient temperatures, indicated with a thick line and gray shading, was calculated according to isotope fractionation equations given by Salomons and Mook (1986) (according to Clark and Fritz, 1997) for the calcite-HCO_3^- ^{13}C exchange reaction and by O'Neil et al. (1969) for

1297 the ^{18}O exchange between calcite and water. No DIC isotope data is available between 1000 and 1600
1298 m depth. Error bars are smaller than the size of the symbols.
1299
1300 Fig. 9. The CH_4/C_2+ ratio vs. carbon isotope composition of CH_4 for the Fennoscandian Shield
1301 samples. Pressurised samples from the Outokumpu Deep Drill Hole (DDH) are highlighted with thicker
1302 rims. SCR refers to sediment covered ridges (Tassi et al., 2012 and references therein) and within the
1303 thermogenic field "II" and "III" refer to type II (oil-prone/marine-sapropelic) and type III (gas-
1304 prone/terrestrial) kerogen, respectively. The suggested field for abiotic CH4 (shaded) includes gases
1305 from the Zambales ophiolite (ZO) and mid-ocean ridges (MOR) (Horita and Berndt, 1999 and
1306 references therein), and artificial CH_4 from bit-metamorphism (Faber et al., 1999). However, CH_4 as
1307 light as -50‰ VPDB from Precambrian Shields has in previous studies been classified abiotic (cf. Fig.
1308 2 and Sherwood Lollar et al., 1993b). Mixing may explain the scatter of data points between the
1309 different blocks, and the isotopic compositions are also subject to fractionation due to oxidation and
1310 isolation/substrate limitation. Data from this study, Jeffrey and Kaplan (1988), Sherwood Lollar et al.
1311 (1993a, 1993b), Haveman et al. (1999) and Pitkänen and Partamies (2007). Diagram modified after
1312 Whiticar (1999).
1313 Fig. 10. Carbon isotopic systematics of CH_4 with depth in the Fennoscandian Shield. Data from this
1314 study, Heikkinen (1972), Hyyppä (1981), Jeffrey and Kaplan (1988), Sherwood Lollar et al. (1993a,
1315 1993b), Haveman et al. (1999), and Pitkänen and Partamies (2007). Pressurised samples from the
1316 Outokumpu Deep Drill Hole (DDH) are highlighted with thicker rims. Isotopic composition of CH_4 in
1317 air is from Mischler et al. (2009). The $\delta^{13}C_{CH4}$ values below -40‰ VPDB are exclusively found in the
1318 upper 1 km depth while values heavier than -20‰ appear to be more common at depths greater than
1319 1.5 km.
1320
1321 Fig. 11. CH_4/C_2+ with depth in the Fennoscandian Shield. Data from this study, Jeffrey and Kaplan
1322 (1988), Sherwood Lollar et al. (1993a, 1993b), Haveman et al. (1999) and Pitkänen and Partamies
1323 (2007). Pressurised samples from the Outokumpu Deep Drill Hole (DDH) are highlighted with thicker
1324 rims. The ratio varies more from site to site than showing shield scale dependence on depth.
1325
1326

1327
1328

1329
1330
1331
1332
1333 Fig. 1
1334
1335
1336

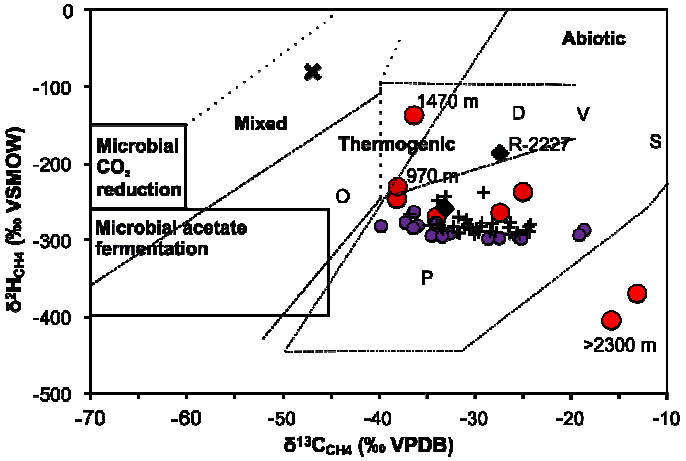

Fig. 2

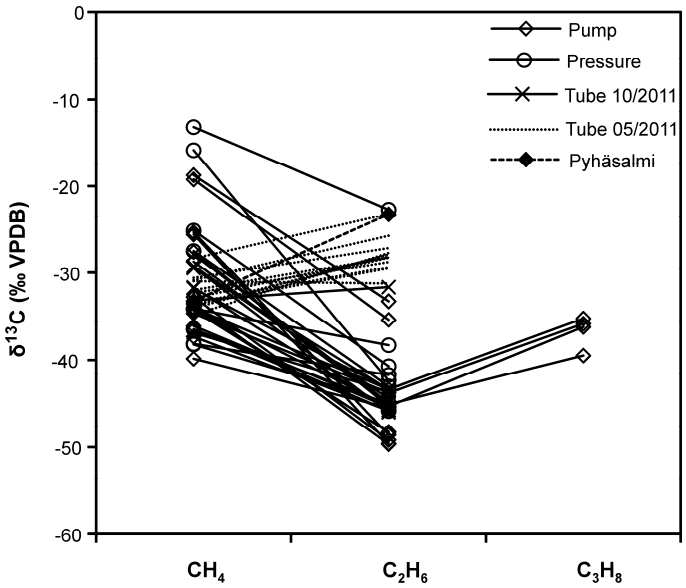

Fig. 3

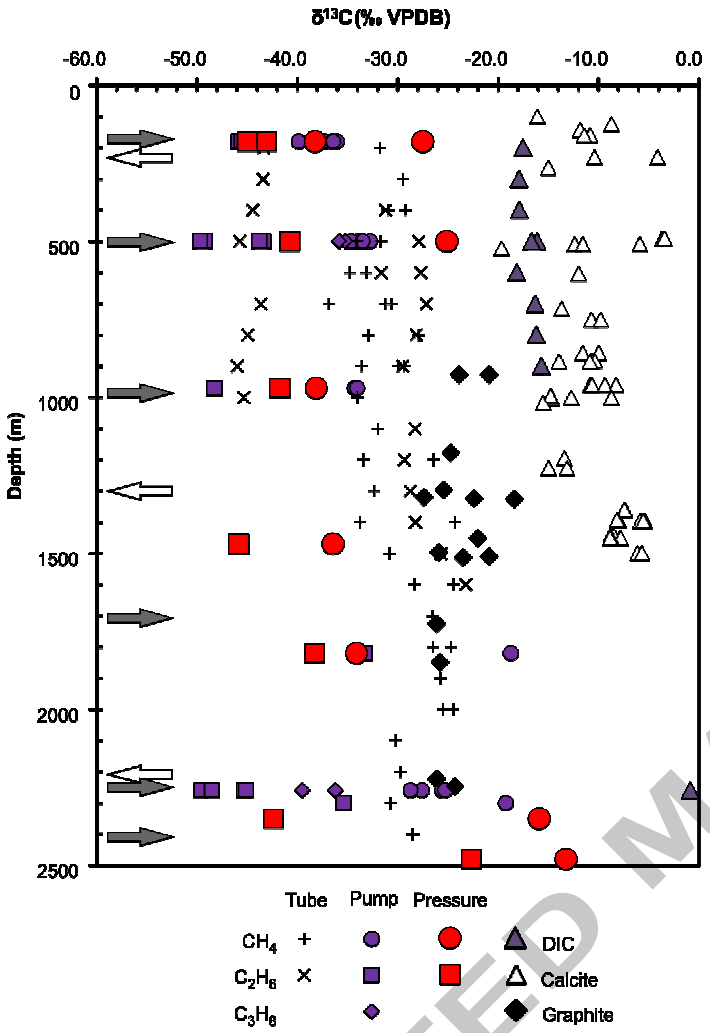

Fig. 4

Fig. 5

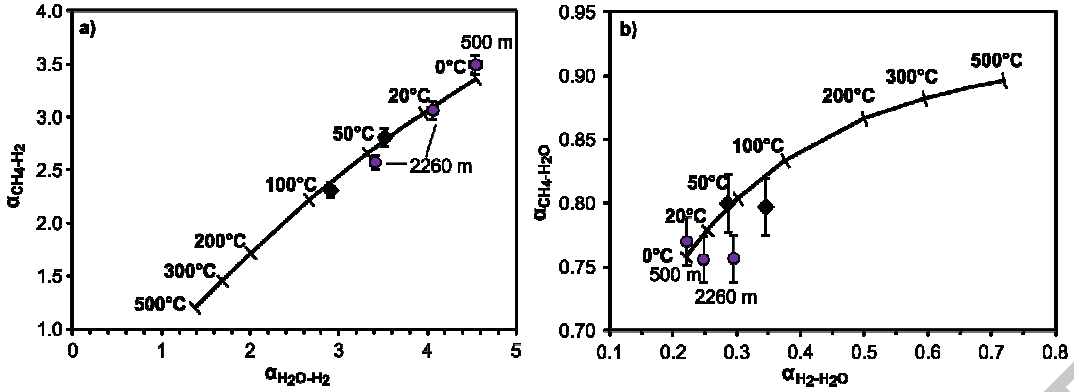

Fig. 6

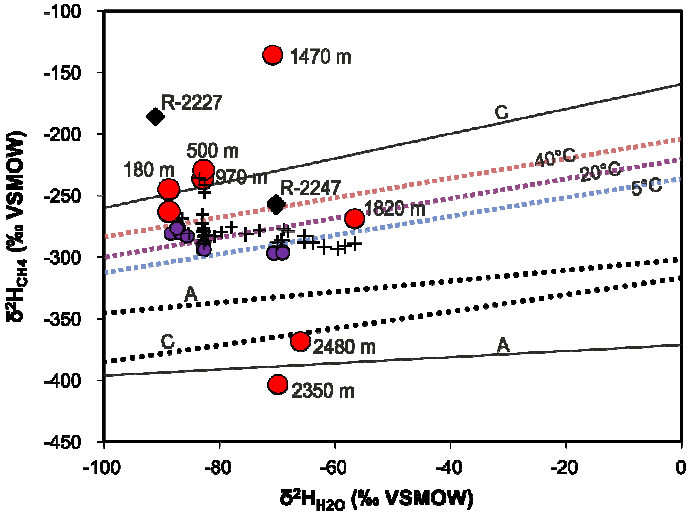

Fig. 7

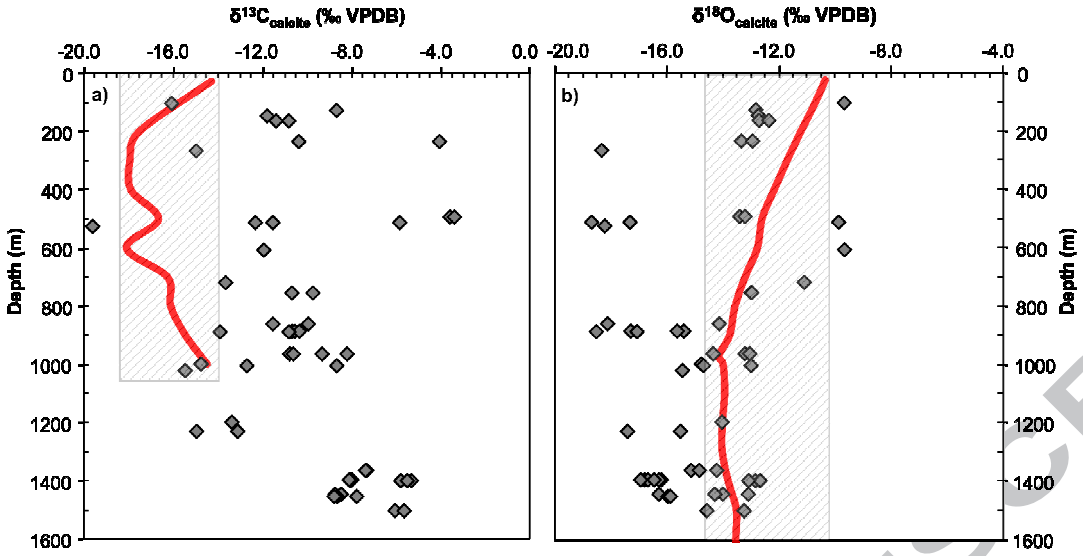

Fig. 8

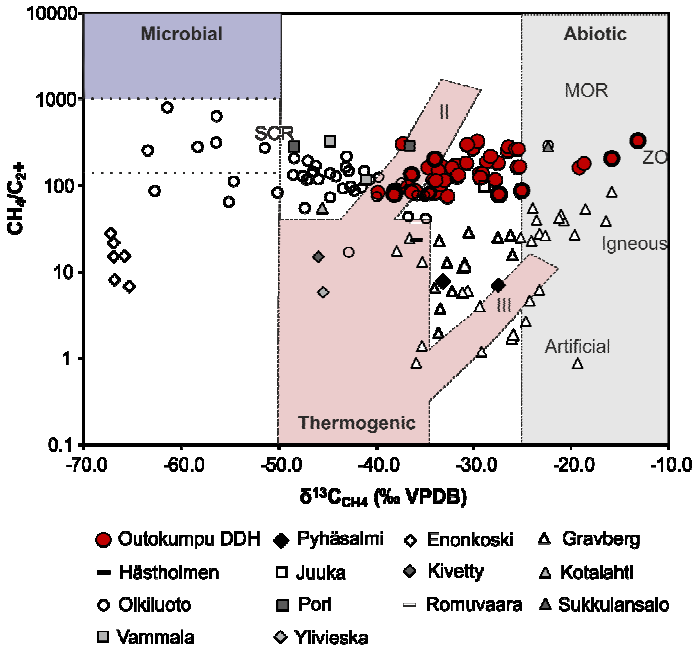

Fig. 9

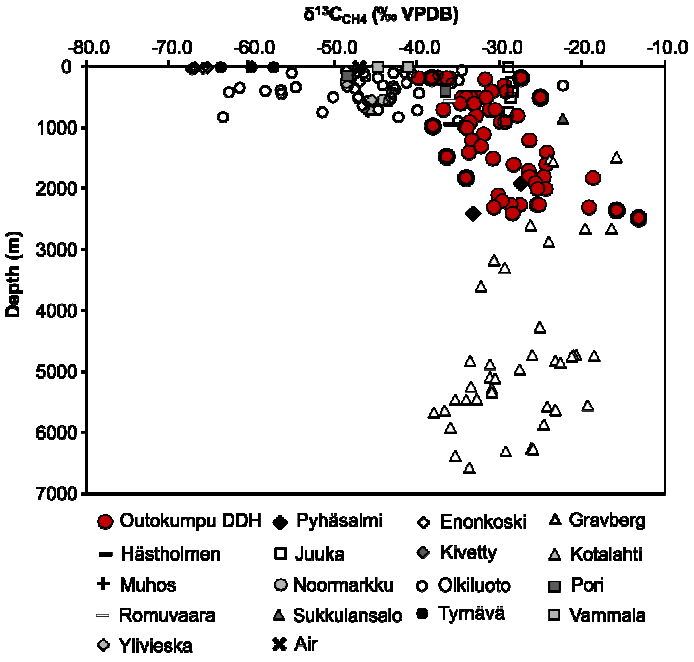

Fig. 10

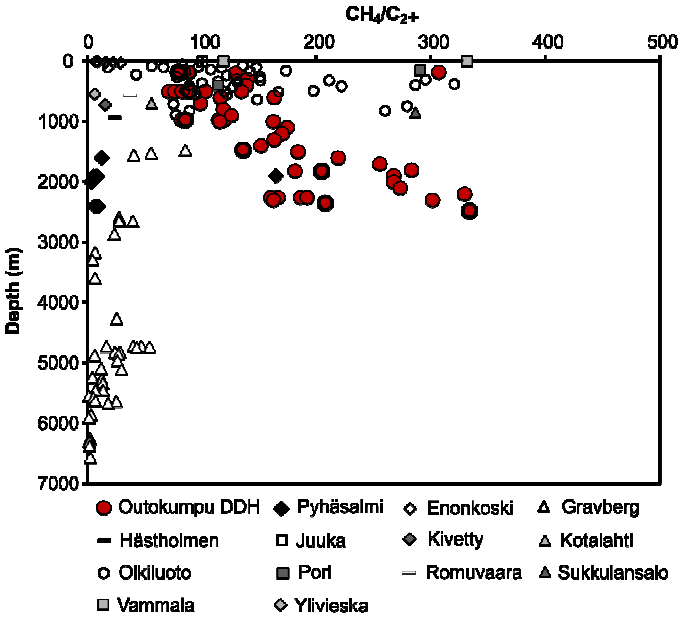

1407

1408

1409

1410 Fig. 11

1411

1412

1413

1414 Table 1.

1415 Fluid sampling campaings in the Outokumpu Deep Drill Hole in 2010-2012.

1416

Date	Method	Depth (m)	Total water volume retrieved (m^3)
27.5.-20.9. 2010	Pumping, one packer at 1190 m depth	2260	6.9
21.9.-9.11. 2010	Pumping between packers at 478 m and 502 m depths	500	9.8
15.-19.5. 2011	Tube sampling	0-2450	0.154
8.-17.6. & 14.7.-2.8. 2011	Direct pumping	2300	3.2
3.-18.8. 2011	Direct pumping	1820	1.0
14.-19.8. 2011	Positive displacement sampler (PDS)	500, 970, 1470, 1820, 2350, 2480	0.0048
5.9.-6.10. 2011	Direct pumping	970	3.8
10.-13.10.2011	Tube sampling	0-1050	0.066
5.5.-18.6. 2012	Pumping between packers at 170 m and 190 m depths & PAVE	180	22.5

1417

1418

Table 2.
Isotopic compositions of methane, ethane, propane, hydrogen, water and dissolved inorganic carbon (DIC) in the Outokumpu Deep Drill Hole and Pyhäsalmi mine, Finland.

Sample	Sampling date	Method[c]	Depth m	CH_4 $\delta^{13}C$ ‰ VPDB	CH_4 $\delta^{2}H$ ‰ VSMOW	C_2H_6 $\delta^{13}C$ ‰ VPDB	C_2H_6 $\delta^{2}H$ ‰ VSMOW	C_3H_8 $\delta^{13}C$ ‰ VPDB	H_2 $\delta^{2}H$ ‰ VSMOW	H_2O[d] $\delta^{2}H$ ‰ VSMOW	H_2O[d] $\delta^{18}O$ ‰ VSMOW	DIC $\delta^{13}C$ ‰ VPDB	DIC[e] mmol l^{-1}
Outokumpu:													
7[a]	8/2008	TSI	700	-31.2	-283					-82.0			
9[a]	8/2008	TSI	900	-29.9	-283					-80.9			
12[a]	8/2008	TSI	1200	-26.4	-276					-78.0			
14[a]	8/2008	TSI	1400	-24.3	-279					-68.2			
16[a]	8/2008	TSI	1600	-24.4	-288					-65.4			
18[a]	8/2008	TSI	1800	-24.7	-287					-69.3			
20[a]	8/2008	TSI	2000	-24.5	-281					-75.5			
Oku Pump 970A[b]	08-09-2009	PI	970	-34.3	-277	-48.2	-240	BAL		-87.5		-24.8	
Oku Pump 970B[b]	08-09-2009	PI	970	-34.0	-277	-48.3	-241	BAL		-87.5		-24.1	
OKU2260-G1	20-06-2010	PI	2260	-27.6	-297	-45.3	BAL	-36.2	-727	-70.7	-10.91		
OKU2260-G3	20-06-2010	PI	2260	-28.7	-297	-45.1	BAL	-39.5	-771	-70.7	-10.91		0.21
OKU2260-G7	28-07-2010	PI	2260	-25.6	-295	-49.6	-239			-69.2	-10.95	-0.8	0.26
OKU2260-G10	28-07-2010	PI	2260	-25.3	-297	-48.6	-235			-69.2	-10.95		
OKU500-G3	30-09-2010	PI	500	-34.0	-292	-43.4	BAL	-35.2	BAL	-82.8	-13.06		0.18
OKU500-G4	30-09-2010	PI	500	-32.8	-291	-49.2	-249			-82.8	-13.06		
OKU500-G8	01-10-2010	PB	500	-34.6	-294	-43.8	BAL	-35.8	-798	-82.9	-13.09		0.08
OKU500-G12	13-10-2010	PB	500	-33.5	-294	-49.7	-247			-82.7	-13.07	-16.1	0.09
OK-5	16-05-2011	TSI	400	-31.0	-273	-31.2	-227			-83.1	-12.85		0.11
OK-6	16-05-2011	TSI	500	-34.1	-279	-27.9	-235			-83.0	-12.89		0.12
OK-7	16-05-2011	TSI	600	-34.8	-280	-27.7	-228			-82.7	-12.93		0.20
OK-8	16-05-2011	TSI	700	-30.6	-282	-27.1	-232			-82.6	-12.96		0.13
OK-9	16-05-2011	TSI	800	-32.9	-287	-28.1	-244			-82.5	-12.97		0.12
OK-11	17-05-2011	TSI	900	-33.6	-283	-29.5	-238			-82.8	-12.92		0.15
OK-12	17-05-2011	TSI	1100	-32.0	-290	-28.3	-246			-82.8	-12.93		0.09
OK-13	17-05-	TSI	1200	-33.4	-286	-29.3	-263			-82.9	-12.79		0.12

OK-14	17-05-2011	TSI	1300	-32.3	-282	-28.7	-270			-82.3	-12.70		0.12
OK-15	17-05-2011	TSI	1400	-33.7	-280	-28.2	-256			-79.7	-12.15		0.14
OK-16	17-05-2011	TSI	1500	-30.9	-279	-25.7	-203			-73.1	-11.23		0.17
OK-17	17-05-2011	TSI	1600	-28.3	-278	-23.2	-243			-68.9	-10.86		0.09
OK-18	18-05-2011	TSI	1700	-26.6	-282	BAL	-225			-60.5	-10.48		0.20
OK-19	18-05-2011	TSI	1800	-26.5	-291	BAL	-239			-58.4	-10.39		0.16
OK-20	18-05-2011	TSI	1900	-25.7	-289	BAL	-233			-56.6	-10.46		0.19
OK-21	18-05-2011	TSI	2000	-25.5	-293	BAL	-276			-59.6	-10.48		0.17
OK-22	18-05-2011	TSI	2100	-30.2	-292	BAL	-226			-61.9	-10.59		0.11
OK-23	18-05-2011	TSI	2200	-29.7	-288	BAL	-223			-63.9	-10.63		0.17
OK-24	18-05-2011	TSI	2300	-30.7	-283	BAL	-225			-65.3	-10.81		0.14
OK-25	19-05-2011	TSI	2400	-28.5	-289	BAL	-251			-70.0	-11.02		0.19

Sample	Sampling date	Method[c]	Depth m	CH_4 $\delta^{13}C$ ‰ VPDB	CH_4 $\delta^{2}H$ ‰ VSMOW	C_2H_6 $\delta^{13}C$ ‰ VPDB	C_2H_6 $\delta^{2}H$ ‰ VSMOW	C_3H_8 $\delta^{13}C$ ‰ VPDB	H_2 $\delta^{2}H$ ‰ VSMOW	H_2O[d] $\delta^{2}H$ ‰ VSMOW	H_2O[d] $\delta^{18}O$ ‰ VSMOW	DIC $\delta^{13}C$ ‰ VPDB	DIC[e] mmol l^{-1}
OKU2300-G1	19-07-2011	PB	2300	-19.2	-293	-35.4	-265			-65.4	-10.56		0.18
OKU1820-G1	17-08-2011	PB	1820	-18.7	-286	-33.3	-254			-56.0	-10.47		0.20
OUTO-500 (6)	28-08-2011	PDS	500	-25.1	-237	-40.7	-265			-82.9	-13.11		0.13
OUTO-970 (2)	25-08-2011	PDS	970	-38.1	-230	-41.8	-277			-82.8	-12.94		0.17
OUTO-1470 (8)	29-08-2011	PDS	1470	-36.4	-136	-45.8	-215			-70.8	-10.84		0.15
OUTO-1820 (4)	27-08-2011	PDS	1820	-34.1	-269	-38.3	-268			-56.6	-10.59		0.20
OUTO-2350 (7)	29-08-2011	PDS	2350	-15.9	-404	-42.4	BAL			-69.9	-11.06		0.21
OUTO-2480 (5)	27-08-2011	PDS	2480	-13.2	-369	-22.7	BAL			-66.0	-11.30		0.17
OU-1	11-10-2011	TSI	25							-84.8	-12.00	-14.3	0.26
OU-3A	12-10-2011	TSI	200	-31.8	-269	-43.4	-242			-86.5	-12.38	-17.5	0.20
OU-4A	12-10-2011	TSI	300	-29.5	-281	-43.4	-234			-85.4	-12.69	-17.9	0.15
OU-5A	12-10-2011	TSI	400	-29.2	-237	-44.5	-249			-83.5	-12.95	-17.9	0.17

OU-6A	12-10-2011	TSI	500	-31.7	-291	-45.8	-218		-82.8	-13.05	-16.7	0.17
OU-7A	12-10-2011	TSI	600	-33.1	-242	-31.6	-221		-82.6	-12.98	-18.1	0.19
OU-8A	13-10-2011	TSI	700	-36.9	-266	-43.6	-223		-83.0	-13.11	-16.2	0.18
OU-9A	13-10-2011	TSI	800	-27.9	-289	-44.9	-238		-83.1	-13.06	-16.2	0.17
OU-10A	13-10-2011	TSI	900	-29.4	-277	-46.0	-230		-82.8	-13.01	-15.7	0.18
OU-11A	13-10-2011	TSI	1000	-34.0	-247	-45.4	-234		-82.6	-13.11	-14.7	0.15
OKU180-G1	05-05-2012	PB	180	-37.3	-276	-45.8	-182		-87.2	-12.54		
OKU180-G2	08-05-2012	PB	180	-36.1	-280	-45.4	-163		-87.0	-12.68		
OKU180-G3	14-05-2012	PB	180	-36.5	-284	-45.1	-194		-85.7	-12.79		0.007
OKU180-G6	05-06-2012	PB	180	-36.5	-263	-45.1	-161		-88.6	-12.57		0.21
OKU180-G7	13-06-2012	PB	180	-39.9	-281	-45.5	-170		-88.4	-12.61		
OKU180/25	18-06-2012	PAVE	180	-27.5	-263	-43.1	-157		-88.8	-12.55		
OKU180/27	18-06-2012	PAVE	180	-38.2	-246	-45.0	-153		-88.8	-12.55		
Pyhäsalmi:												
PYS-1B/R2247	11-06-2014	FFI	2400	-33.2	-259	-23.2	BAL	-680	-70.2	-12.27		0.003
PYS-1C/R2247	11-06-2014	FFI	2400	-33.3	-256	-23.2	BAL	-736	-70.2	-12.27		
PYS-2B/R2227	11-06-2014	FFI	1910	-27.5	-186				-91.2	-13.70		0.0005

[a] Data from Nyyssönen et al. 2014

[b] Data from Toppi 2010

[c] Sampling methods: TSI = tube sampling/injection, PI = Pumping/injection, PB = pumping/bucket, PDS = positive displacement sampler, PAVE = pressurised sampling device, FFI= from free flowing fluid/injection.

[d] Data from Nyyssönen et al. 2014, Toppi 2010, Kietäväinen et al. 2013, Miettinen et al. 2015 and this study.

[e] The concentration of dissolved inorganic carbon was modelled based on geochemical data with PHREEQC software (USGS, 2014)

BAL = below analytical limit

Table 3.
Carbon and oxygen isotopic compositions of fracture/vein calcites from the Outokumpu Deep Drill Hole.

Sample ID	Depth m	Calcite type and position	Orientation[a]	$\delta^{13}C$ ‰ VPDB	$\delta^{18}O$ ‰ VPDB
47	100.90	Platy, open fracture	V	-16.10	-9.7
48	124.80	Massive	?	-8.71	-12.9
50	143.51	Platy, blocky	H	-11.82	-12.8
1	160.80	Blocky, euhedral	V	-10.85	-12.7
2	160.80*	Blocky, euhedral	V	-11.42	-12.4
3	231.80	Platy, flaky, surface 1	V	-10.40	-13.4
4	231.80	Platy, flaky, surface 2	V	-4.10	-13.0
52	263.95	Blocky, open fracture	H	-15.00	-18.4
5	490.70	Thin film	V	-3.63	-13.4
6	490.70*	Thin film	V	-3.43	-13.2
7	510.00	Platy, blocky, coarse	H	-12.35	-18.7
8	510.00*	Platy, blocky, coarse	H	-11.56	-17.3
9	510.00	Flaky, film	V	-5.88	-9.9
54	523.15	Platy, coarse	O	-19.64	-18.2
10	604.85	Powdery	V	-11.97	-9.7
55	716.35	Thin film	V	-13.68	-11.1
56	751.80	Thin film	O	-10.71	-13.0
57	751.80	Massive, upper	O	-9.77	-13.0
58	858.50	Blocky	V	-11.56	-14.2
59	858.50	Massive	V	-9.98	-18.1
11	883.60	Box shaped, subhedral	O	-10.70	-15.4
11B	883.60	Box shaped, euhedral	O	-10.58	-15.7
12	883.60	Platy, blocky, vein	O	-10.38	-17.3
13	885.75	Platy, bent, lower	V	-13.93	-18.5
14	885.75	Massive, upper	V	-10.84	-17.1
15	961.25	Massive, very hard, upper	V	-9.36	-13.2
16	961.25	Massive, very hard, central	V	-10.81	-14.4
17	961.25	Massive, lower	V	-10.65	-13.1
18	961.25	Massive, soft	H	-8.24	-14.4
60	996.20	Massive	O	-14.78	-14.8
19	1001.90	Platy, open fracture	V	-12.73	-14.7
20	1001.90*	Platy	V	-8.70	-13.0
21	1018.60	Powdery	V	-15.49	-15.5
22	1195.70	Powdery	V	-13.40	-14.1
23	1227.20	Box shaped, subhedral	V	-13.14	-15.5
24	1227.20*	Box shaped, subhedral	V	-14.98	-17.4
25	1361.25	Box shaped, vein, central	H	-7.36	-15.2
26	1361.25*	Box shaped, vein, central	H	-7.36	-14.9
27	1361.25	Box shaped, vein, lower	H	-7.41	-14.3
28	1393.67	Needles, upper	O	-8.12	-16.8
29	1393.67	Powdery, lower	O	-8.08	-16.2
30	1393.67	Elongated, upper	O	-8.03	-16.3
31	1393.67	Elongated, upper-central	O	-8.08	-16.7
32	1393.67	Elongated, lower-central	O	-8.02	-16.5
33	1393.67	Elongated, lower-central	O	-8.14	-17.0
34	1396.48	Massive, soft, vein 1, upper	O	-5.83	-12.9
36	1396.48	Massive, vein 2, upper	O	-5.36	-12.7
37	1396.48	Massive, vein 2, lower	O	-5.54	-13.1
38	1442.95	Massive, thin vein	V	-8.78	-13.1
39	1442.95	Box shaped, vein, upper	V	-8.78	-14.0

40	1442.95	Box shaped, blocky, vein, central	V	-8.50	-16.3
41	1442.95	Box shaped, vein, lower	V	-8.50	-14.3
42	1450.75	Massive, vein	V	-7.81	-16.0
43	1450.75	Massive, vein, lower	V	-8.69	-15.9
44	1450.75	Massive, vein, central	V	-8.82	-15.9
45	1499.35	Powdery	V	-6.09	-14.6
46	1499.85	Blocky, vein	H	-5.68	-13.3

[a]= V: vertical, H: horizontal, O: oblique
* = duplicate sample